MASTERARBEIT | MASTER'S THESIS

Titel | Title

The impact of chemically induced oxidative stress and mechanical cues on mechanosensitive transcription factors in ovarian cancer cells

verfasst von | submitted by

Sarah Angela Younan BSc

angestrebter akademischer Grad | in partial fulfilment of the requirements for the degree of

Master of Science (MSc)

Wien | Vienna, 2025

Studienkennzahl lt. Studienblatt | Degree programme code as it appears on the student record sheet:	UA 066 862
Studienrichtung lt. Studienblatt | Degree programme as it appears on the student record sheet:	Masterstudium Chemie
Betreut von | Supervisor:	Ass.-Prof. Dott. ric. Giorgia Del Favero Privatdoz.

Acknowledgements

First and foremost, I would like to express my gratitude towards Ass. Prof. Dott. Ric. Giorgia Del Favero for giving me the opportunity of working in her research group. Not only was I introduced to the beautiful world of immunofluorescence microscopy, but I also got to work on a project that reignited my passion for scientific research. A big thank you goes out to Maximilian Jobst MSc. for his continuous support throughout my Master Thesis, guiding me through all experiments and the evaluation, as well as a multitude of intellectual discussions about science, coffee, video games and cheese. Thank you to Dr. Martina Karasová for teaching me how to work with ovarian cancer cells, showing various hacks in the lab and sharing her broad knowledge (and amazing baked goods) with me. I am grateful for Janice Bergen MSc. for always willing to help me whenever a miscellaneous question or problem arose. In general, I want to say thank you to everyone in the Del Favero group for being so welcoming and making my time working there an unforgettable experience.

My deepest gratitude goes to my mother Claudia and my brother Raphael for their endless support throughout my life. To my best friends Pauline and Jana, for always being there for me – celebrating the highs and catching me during the lows of life. To my first university friend Claudia and all the lovely friends I made along the way, who made study days fun, lab courses bearable and the past years unforgettable.

This work was supported by the Austrian Science Fund (FWF) [Grant-DOI 10.55776/P35822]

Contents

Abstract

Ovarian cancer (OC) is one of the deadliest gynecological malignancies, driven by its unspecific symptoms, high heterogeneity among subtypes and ability to acquire chemoresistance. Gaining a deeper understanding of what contributes to this aggressive phenotype is therefore of relevance to improving treatment prognosis. The tumour microenvironment (TME) of OC is characterized by high levels of oxidative stress (OS) as well as dynamic mechanical stimuli, amongst others. Therefore, investigating these chemical and mechanical stressors is of interest, as they seem to play a role in shaping the OC phenotype. One way these cells adapt is through altering OS responsive key molecular signalling pathways such as the Keap1/Nrf2/ARE pathway, known for its main function of increasing antioxidant defenses. Therefore, the aim of this thesis was to investigate how chemically and mechanically induced OS impacts the cellular behavior and viability of epithelial OC cells in terms of the expression and translocation of the mechanosensitive transcription factors (TF) Nuclear factor erythroid 2-related factor 2 (Nrf2), as well as the potential role of Krüppel-like factor 2 (KLF2) in priming this antioxidant response. The epithelial OC cell lines SKOV3 and OVCAR3 were subjected to physiologically relevant levels of H_2O_2 in isolation and in combination with 1 h of fluid shear stress (FSS) and assessed for TF translocation and cell viability. For both cell lines, fluorescence microscopy and image analysis revealed a concentration dependent increase in nuclear translocation of Nrf2. Additionally, mechanical stimulation via SS was also found to promote Nrf2 activation, whereas KLF2 translocation was only observed in SKOV3 cells. Cell viability assays revealed a decrease in cytotoxic potential under high OS conditions in both ovarian cancer subtypes when co-exposed to SS, suggesting a functional Nrf2 mediated antioxidant response. The potential involvement of KLF2 in this response could be postulated for SKOV3 cells, whereas OVCAR3 cells seem to rely on more complex mechanisms dependent on perceived stress intensity. Taken together, the obtained findings underscore the relevance of Nrf2 as a central regulator to functional OS adaptation in epithelial ovarian cancer. The results indicate differential stress adaptation strategies employed by the two cell lines, highlighting the heterogeneous phenotype of OC. The findings emphasize the importance of investigating components of the TME not in isolation but as interconnected cues that shape the behaviour of OC cells.

Zusammenfassung

Eierstockkrebs ist eine der tödlichsten gynäkologischen Erkrankungen, was zum Teil auf unspezifische Symptomatik, Heterogenität zwischen den Subtypen und die Fähigkeit chemoresistent zu werden basiert. Um die Behandlungsprognose zu verbessern ist es deshalb von Relevanz, ein tieferes Verständnis von den zugrundeliegenden molekularen Mechanismen zu erlangen, welche zu diesem aggressiven Phänotyp beitragen. Die Tumormikroumgebung (TME) von Ovarialkarzinomen ist unter anderem durch ein hohes Maß an oxidativem Stress (OS) sowie dynamischen mechanischen Stimuli gekennzeichnet. Diese chemischen und mechanischen Faktoren beeinflussen das Verhalten und die Anpassungsfähigkeit von Eierstockkrebs, indem sie molekulare Signalwege verändern, die auf OS reagieren. Im Rahmen dieser Arbeit wurde deshalb der Fokus auf den Keap1/Nrf2/ARE Signalweg gelegt, welcher bekannt für die Aktivierung von intrazellulären Verteidigungsmechanismen als Antwort auf OS ist. Genauer gesagt wurde untersucht, wie OS das zelluläre Verhalten von epithelialen Eierstockkrebszellen in Bezug auf die Expression und Translokation des Transkriptionsfaktors (TF) Nrf2 beeinflusst, sowie ob mechanische Stimuli und der TF KLF2 bei der Signalauslösung dieser antioxidativen Reaktion beteiligt sind. Dazu wurden die epithelialen Eierstockkrebszelllinien SKOV3 und OVCAR3 physiologisch relevanten Konzentrationen an H_2O_2 sowohl isoliert als auch in Kombination mit einstündiger Scherspannung („Fluid shear stress“, SS) ausgesetzt und auf TF-Translokation und die Überlebensfähigkeit der Zellen untersucht. Fluoreszenzmikroskopie und Bildanalyse zeigten in beiden Zelllinien eine konzentrationsabhängige Zunahme der nukleären Translokation von Nrf2. Darüber hinaus führte die mechanische Stimulation durch SS ebenfalls zu einer Aktivierung von Nrf2, während eine Translokation von KLF2 ausschließlich in SKOV3-Zellen beobachtet wurde. Zellviabilitätsassays zeigten eine Abnahme des zytotoxischen Potenzials unter hohen OS-Bedingungen bei beiden Eierstockkrebs Subtypen, wenn sie gleichzeitig SS ausgesetzt waren, was auf eine funktionelle Nrf2-vermittelte antioxidative Antwort hindeutet. Für SKOV3-Zellen könnte zudem die potenzielle Beteiligung von KLF2 in dieser funktionellen Anpassungsfähigkeit postuliert werden, wohingegen OVCAR3-Zellen eher auf komplexere, von der Stressintensität abhängige Anpassungsmechanismen zurückgreifen. Insgesamt unterstreichen die erhaltenen Ergebnisse die zentrale Rolle von Nrf2 als Regulator der zellulären Anpassung an OS im epithelialen Ovarialkarzinom sowie die mögliche Beteiligung von KLF2 als Antwort auf mechanische Stimuli. Die erzielten Ergebnisse deuten auf unterschiedliche Stressanpassungsstrategien der beiden Zelllinien hin und unterstreichen den heterogenen Phänotyp von Eierstockkrebs. Die Ergebnisse unterstreichen, wie wichtig es ist, die Komponenten der TME nicht isoliert, sondern als miteinander verbundene Signale zu untersuchen, die das Verhalten von Eierstockkrebszellen beeinflussen.

Abbreviations

ARE	Antioxidant response element
CAM	Cell adhesion molecule
CAT	Catalase
CCC	Clear cell carcinoma
CTB	CellTiter™ blue
Cul3	Cullin-3
DMEM	Dulbecco's Modified Eagle Medium
DMSO	Dimethyl sulfoxide
EC	Endometroid carcinoma
eNOS	Endothelial nitric oxide synthase
EOC	Epithelial ovarian cancer
ETC	Electron transport chain
FCS	Fetal calf serum
FSS	Fluid shear stress
GSH	Glutathione
GST	Gluthathione-S-transferase (GST)
HGSOC	High-grade serous ovarian carcinoma
HP	Hydrostatic pressure
HUVECS	Human Umbilical Vein Endothelial Cells
Keap1	Kelch-like-associated protein 1
KLF2/4	Krüppel-like factor 2/4
LGSOC	Low-grade serous ovarian carcinoma
NAD(P)H	Nicotinamide adenine dinucleotide phosphate
NOXs	NADPH oxidases
Nrf2	Nuclear factor erythroid 2-related factor 2
OS	Oxidative stress
P/S	Penicillin and Streptomycin
PBS	Phosphate buffered saline solution
RNS	Reactive nitrogen species
ROS	Reactive oxygen species
sMaf	Small musculoaponeurotic fibrosarcoma proteins
SOD	Superoxide dismutase
SS	Shear stress
TF	Transcription factor
TME	Tumour microenvironment
TTX	Triton X-100

1 Introduction

1.1 Ovarian cancer

1.1.1 Epidemiology and aetiology

Ovarian cancer (OC) is the seventh most common type of cancer in women worldwide, with more than 225.500 new diagnoses being recorded every year. While breast cancer remains the most predominant type of female reproductive tumours, ovarian cancer is the one with the highest lethality rate, having a survival rate after 5 years of around 47.4%.[1] It is oftentimes referred to as the "silent killer", since the early stage symptoms are very unspecific, with 70% of diagnoses occurring when the carcinoma has already progressed to advanced stages or spread to other organs, lowering the success of therapeutic interventions. While the likelihood of developing ovarian cancer in women under the age of 30 is low, increased age is proportionally correlated to increased risk, particularly in the demographic group of postmenopausal women. Multiple factors contribute to the increased incidence of developing OC, including genetic predispositions, reproductive factors, hormonal contraceptives and hormonal replacement therapy amongst others.[2] For example, for women who have a genetic mutation in the tumour suppressor genes BRCA1 and BRCA2 the risk of developing OC is increased to 20-40% and 10-20% respectively compared to the risk being <2% for the general female population.[3] Additionally, other lifestyle-related factors such as physical activity, tobacco-use or diet as well as a medical history of gynaecological disorders like ovarian cysts or endometriosis all contribute to an increased likelihood of developing OC.[4] On the other hand, there are also various factors that are linked to be protective in terms of developing OC such as pregnancy or breastfeeding. The most important one from a public health perspective is however the use of oral contraceptives, being associated with an overall estimated protection of around 25-30%. These protective effects increase with the duration of use and persist for over 30 years after ceasing the usage.[5] The reason for this is suspected to be due to hormonal changes as well as a decrease in the total number of ovulatory cycles a woman goes through throughout her life, as fewer numbers are associated with a lowered risk.[4,6]

1.1.2 Classification

Another aspect that contributes to the lethality of OC is the broad heterogenicity of the cancer.[7,8] Generally, the classification of OC can be divided into three subtypes, namely epithelial, germ-cell and sex-cord-stromal.[1] The most common type of ovarian cancer is of the epithelium, making up around 95% percent of all diagnoses, with the remaining 5% being accounted for the latter two subtypes.[9] Epithelial malignancies can have multiples sites of origin, such as the ovaries themselves, but also the fallopian tube and other epithelial sites in the pelvis. There exist five different subtypes of epithelial ovarian cancer (EOC) which are commonly categorized based on their

histological classification. This includes high and low grade serous ovarian cancer, clear cell-, endometrioid- and mucinous carcinomas, as can be seen in the following figure (***Fig.1***).[10]

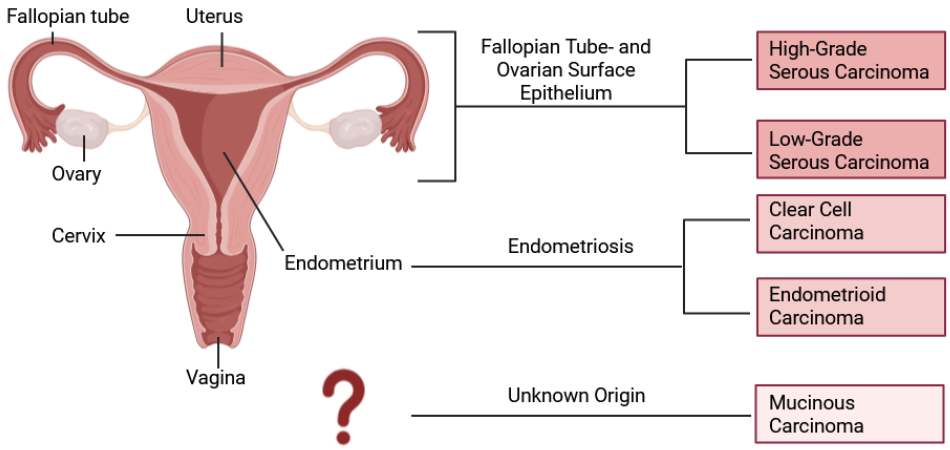

Figure 1: Anatomy of the uterus and classification of OC subtypes; Created using biorender.com; Information compiled from various sources.[1,5,7,8]

High grade serous ovarian cancer (HGSOC) is the most common type of epithelial ovarian carcinoma, making up around 75% of all endothelial ovarian cancers. It is characterized by a very heterogeneous growth pattern as well as mutations in the DNA repair pathways, resulting in increased cell survival and growth.[11] Low grade serous ovarian cancer (LGSOC) is the second most frequent subtype with around 10% of classifications. Contrary to HGSOC, this type less aggressive in terms of growth speed with the cells also being more well-differentiated.[12] This is also reflected in the prognosis, with the overall survival rate of LGSOC being 99 months compared to 57 months of HGSOC.[13] Clear cell carcinomas (CCC) make up around 10% of EOC and usually have a relatively good prognosis, as around 50% of cases are detected in earlier stages. They are sought to originate from endometriosis, with their histological characteristic being the presence of clear cytoplasm. The second type of EOC associated with endometriosis is endometroid carcinomas (EC). Similarly to CCC, this histological subtype seems to be chemosensitive when detected in earlier stages, resulting in a better prognosis.[1,8] Mucinous carcinoma (MC) is the rarest type of EOC, and it is oftentimes associated with metastasis stemming from the gastrointestinal, biliary tract or the pancreas. For the treatment of this subtype the stage of cancer upon diagnosis is of importance, because while earlier stages are well treatable, advanced MC prognosis outcomes are very poor.[8] Furthermore, smoking, obesity, endometriosis and nulliparity contribute to the likelihood of developing EOC.[11]

Another well-established way of categorizing EOC is into their level of lethality, either being grouped into type 1 or type 2. Type 1 EOC include LGSOC, CCC and MC, with characteristics being that they are genetically more stable and are usually detected at earlier stages, thus having better treatment prognosis and a lower lethality rate. On the other hand, type 2 includes HGSOC and is sought to be more aggressive in its pathogenesis. They express aberrant mutations of tumour suppressor genes such as p53 and BRCA, and are usually detected at more advanced

stages and hence being correlated to a high lethality rate.[1,14] Although the general circumstances surrounding the tumorigenesis of OC is still poorly understood, it sought to most likely originate from the ovarian surface epithelium.[6]

1.1.3 Therapy approaches

As of now, the current therapy approaches depend vastly on the stage of the cancer as well as the histological and molecular profile of the tumour. The traditional front-line procedure is the performance of cytoreductive surgery, typically followed by intravenous chemotherapy.[15] The most widely applied chemotherapeutics are hereby platinum-based drugs such as cisplatin or carboplatin. In case of early-stage OC that is still confined to the ovaries, the primary treatment only involves surgical removal of the affected ovary and fallopian tube, omitting the use of chemotherapeutic drugs.[7] However, if the disease stage is already advanced, more multi-modal approaches are applied. Hereby, the main method of procedure commonly involves a combination of adjuvant chemotherapy and cytoreductive surgery.[1,8] The reason for the deployment of chemotherapeutics is that complete debulking of the tumour at this stage is oftentimes not feasible, as it has oftentimes spread to other tissues in the pelvis or abdomen. Therefore, induction chemotherapy is oftentimes the first-line approach in order to decrease tumour size, and in case there is a response to the drugs, sectional debulking of the tumour can be performed.[4,7] Platinum-based compounds in combination with paclitaxel are usually deployed, inducing DNA damage to cancer cells, with initial response rates being high. Precisely, around 80% of treated patients exert a complete response to the front-line treatment. Unfortunately, the reoccurrence rate for OC is high, which is oftentimes accompanied by increased chemoresistance. This seems to apply to around 75-80% of women who achieved remission, particularly those who had suboptimal debulking or were in more advanced stages of the cancer, as a reoccurrence of EOC was observed within 18 months.[4,16,17]

The chemoresistance of OC can arise from a variety of different mechanisms, such as enhanced DNA repair or altered cell survival pathways, which is the major reason as to why the mortality rate is so high.[11] Another aspect that seems to complicate the treatment is the heterogenicity of OC, as each type has specific characteristics as to how they respond to therapy methods including chemosensitivity.[17] Therefore, it has been proposed to plan therapy approaches on the different types rather than the stage of cancer. Overall, understanding the heterogenicity and mechanisms of drug resistance in OC is of relevance for improving disease management.[4] In recent years, there has been an increased focus on the role of the tumour microenvironment (TME) and cancer cell stress adaptation mechanisms in OC progression and therapy resistance. In this regard, cellular responses to oxidative stress (OS) as well as the impact of mechanical forces have been emerging as important areas of investigation.[18] Signalling pathways involved in the mediation of reactive oxygen species (ROS) are being investigated in regard to potential targets for OC treatments. Particularly, the Keap1-Nrf2-ARE pathway has been emerging as a promising target, as it is one of the main mechanisms linked to keeping the intracellular redox state in homeostasis.[19] Nrf2 in particular has been subject of interest in toxicology and disease over decades due to its role in resistance to OS,

being the master regulator of cytoprotective and antioxidative systems.[19–21] Alterations of this pathway have been reported to be involved in the formation of malignancies, increased survival rate of carcinomas as well as chemoresistance.[22] Additionally, as the peritoneal cavity is an environment characterized by a variety of mechanical cues, signalling pathways that are responsive to such physical stimuli are another target to be investigated.[23] Ultimately, the goal would hereby be to find potential vulnerabilities or novel targets to improve the current state of therapy.[4] Therefore, the following chapters will elucidate the role, function and relevance of OS and mechanical cues, with a particular focus on the involvement of mechanosensitive transcription factors Nrf2 and KLF2 in OC pathogenesis.

1.2 Oxidative stress, ROS and antioxidants

Oxidative stress (OS) can be defined as a disbalance between pro-oxidants and anti-oxidative defences in the body, shifting cells out of their homeostatic state into a more oxidizing environment.[21] Such a disbalance can be caused through the generation of free radicals, triggered by both endogenous and exogenous factors. Amongst the endogenous factors, the mitochondria is the primary site of ROS generation under physiological conditions, where they are produced as natural byproducts of the electron transport chain (ETC).[24,25] During the oxidative phosphorylation, a small fraction of electrons can leak from the complexes 1 and 3 from the ETC, causing the generation of superoxide anions (O^{2-}).[26] Other sources of cellular ROS include enzymatic systems such as NADPH oxidases (NOXs) as well as inflammatory responses.[27] Exogenous sources like ultraviolet radiation or environmental contaminants also contribute to the amplification of OS onto cells.[20,28] In the physiological system, the excessive production of ROS or reactive nitrogen species (RNS) is reflected as an increase in perceived cellular stress.[27] Under normal conditions, cells employ a complex network of antioxidant mechanisms to maintain redox homeostasis. However, when the level of such pro-oxidative molecules exceeds a point where the intracellular antioxidant system cannot counteract accordingly, it leads to a state of OS in the cells.[26] Consequently, cells experience irreversible damage to proteins, lipids and nucleic acids, leading to the interference with various cellular functions.[18]

OS has been proven to be closely correlated to the occurrence and development of a variety of diseases, such as Alzheimer's disease[29], Diabetes mellitus[30] and notably cancer.[28] It is involved at many stages of the oncogenic process, such as the initiation, promotion and progression of a carcinoma.[31] In cancer cells, the redox homeostasis is significantly altered compared to healthy cells, playing a dual role. On one hand, increased levels of ROS are correlated to genomic instability and mutations, being linked to initiating tumorigenesis.[28,32] For example, chronically elevated levels of OS in the ovaries have been suggested to be involved in the early transformation of surface epithelial cells.[31] On the other hand, once a tumour is established, the cells seem to thrive under elevated levels of OS. The increased production of ROS promotes various mechanisms, such as influencing the regulation of genes and affecting the intracellular signalling pathways.[33] For example, research shows that ROS induce the activation of various pathways involved in cell division, such as MAPK, PI3K and AKT.[34] This shift in redox

balance towards the oxidative state has been linked to accelerated proliferation, as well as more rapid and aggressive growth of cancer cells.[33] However, to withstand the high amount of intracellular ROS that would drive regular cells towards senescence and apoptosis, cancer cells have adapted over time by developing mechanisms that counteract OS. One way that carcinomas resolve this is by overexpressing antioxidant biochemical pathways. This adaptation alters the baseline redox homeostasis of the cancer cell, increasing its ability to withstand higher levels of OS, preventing the onset of cytotoxicity.[28,33] This is for example achieved through the activation of molecular signalling cascades such as the Keap1-Nrf2-ARE pathway, resulting in the upregulation of antioxidant enzymes such as in the glutathione system.[19,35]

1.2.1 Reactive oxygen species and the relevance of H_2O_2:

ROS is an umbrella term encompassing a multitude of oxygen-based derivatives originally known for their ability to oxidize organic substances. Generally, they can be divided into non-radical species, such as hydrogen peroxide (H_2O_2), organic hydroperoxides (ROOH) and singlet molecular oxygen ($^1O_2$), and free radicals like the superoxide anion - (O^{2-}), hydroxyl (·OH) - or peroxyl (ROO·) - radical.[27,33] In biological systems, ROS play a vital role in the physiology and cellular signalling mechanisms, with hydrogen peroxide (H_2O_2) being a being a major signalling agent (***Fig.2***). Physiological levels of H_2O_2 are in the range of approximately 1-100 nM in the cells and, together with reactive nitrogen species (RNS), are naturally occurring byproducts of cellular metabolism. They are mainly generated during cellular respiration that is taking place in the mitochondria.[18] While stimuli such as metabolic cues, but also physical stressors and chemokines can increase intracellular H_2O_2 levels, reducing agents (i.e. catalase[36]) counteract this, ensuring that ROS levels remain at physiological levels. The maintenance of intracellular low concentrations of H_2O_2 can be referred to as oxidative eustress and it is involved in the signalling of various processes such as proliferation, migration and differentiation of cells. However, a disbalance in the redox signalling can lead to elevated levels of H_2O_2 (>100 nM), which is oftentimes referred to as oxidative distress. It is correlated to the expression and initiation of a variety of cellular responses that lead to effects such as inflammation, cell growth arrest or cell death.[27]

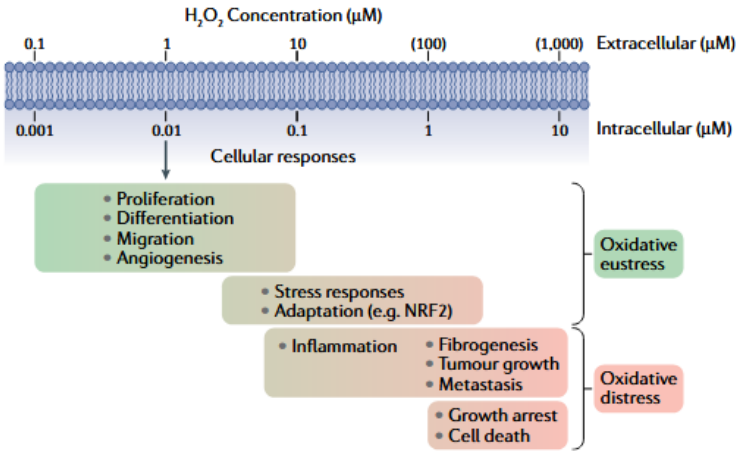

Figure 2: Cellular responses to physiological levels of H_2O_2: Oxidative eustress and distress[27]

1.2.2 Antioxidants and Nrf2:

While ROS and free radicals are what shifts the cells towards a pro-oxidative state, antioxidants are on the other side of the redox balance, trying to keep the homeostatic state of the cells intact.[26] In general, the antioxidant defence system can be divided into two groups, namely the enzymatic and non-enzymatic ones.[28] Hereby, the primary response of cells is mediated through enzymatic antioxidant systems, such as for instance the conversion of superoxide into H_2O_2 through superoxide dismutases (SOD) followed by the decomposition of H_2O_2 to H_2O through catalase (CAT)[25] or glutathione peroxidases. Non-enzymatic antioxidants include vitamins (A,C,E), glutathione (GSH) and flavonoids, which are molecules that primarily function by scavenging ROS.[18] In principle, the strategy of antioxidants is to promote the cellular defence by increasing the capacity of detoxifying oxidants or by acting as scavengers for free radicals to protect the cells from being damaged.[37] Under normal physiological conditions, these mechanisms are what keeps the redox state of the cells at homeostasis. However, the overexpression of antioxidant pathways is one way through which tumour cells survive in high ROS environments.[31] The induction of antioxidant enzymes in response to OS is highly sensitive, with various transcription factors being known to be involved in the alteration of redox signalling in cancer cells. For example, NF-κB (Nuclear Factor kappa-light-chain-enhancer of activated B-cells) was shown to promote the expression of antioxidant enzymes glutamate-cysteine ligase and SOD.[38,39] One of the most relevant transcription factors when it comes to the induction of antioxidant genes is Nrf2, making it a key player in terms of cellular redox signalling.[37]

The nuclear factor erythroid 2-related factor 2 (Nrf2) is a transcription factor that is regarded the master regulator of OS response. It belongs to the subfamily of cap 'n' collar subfamily of basic region leucine zipper transcription factors and it was first discovered in 1994 regulating the transcription of beta-globin.[37,40] It is involved in multiple cellular phase I, II and III detoxifying processes, highlighting its main role in in biological systems to resist oxidative damage. While Nrf2 can be activated through multiple pathways, such as MAPK signalling molecules or mechanical cues, it is primarily known to respond to OS.[20,41,42] In the context of oncology, Nrf2 can be viewed as a double-edged sword. On one side, the activation of this transcription factor and the therefore resulting expression of antioxidant genes can protect cells from incoming damage. Thus, Nrf2 is often referred to for its role as a tumour suppressor.[22] Contrary to that, this cytoprotective quality of Nrf2 could play a role in the survival of cancer cells. Tumour cells are oftentimes characterized by a multitude of genetic modifications and an increased state of OS.[43] Thus, cancer cells oftentimes show an overexpression of Nrf2 which is frequently accompanied by a high degree of drug resistance, impeding therapeutic approaches.[44] As a result, the modulation of Nrf2 as a therapeutic target has gained considerable attention in recent years.[45]

One of the most important pathways through which cells respond to OS is the Keap1-Nrf2-ARE pathway.[20] The general mechanism under with this signalling pathway works under constitutive and OS conditions can be seen in the following figure (***Fig.3***). Under basal conditions, the expression of Nrf2 is sequestered by Kelch-like-associated protein 1 (Keap1), which is a cysteine-rich repressor protein mainly found in the cytoplasmic area of

cells.[46] Nrf2 can be divided into six highly conserved domains, namely Neh1 to Neh6, of which Neh2 was shown to mediate the binding with Keap1.[47] In particular, the binding of this domain takes place at the β-propeller (Kelch) structure of Keap1.[48] It forms a dimer complex with cullin-3 (Cul3) called the E3 ubiquitin ligase complex. This binding facilitates the ubiquitination of Nrf2, subsequently resulting in polyubiquitination and subsequently the degradation of this TF by the 26S proteasome.[21,49] The sequestration of Nrf2 can be interrupted through various mechanisms, of which one is in the presence of oxidative stressors such as electrophiles and ROS.[50] Electrophiles caused by for example ROS interfere with the binding sites of the Keap1 complex with Nrf2. Precisely, human Keap1 contains multiple cysteine residues that are oftentimes located near basic amino acids, making them favourable targets for electrophiles.[50,51] Hereby, depending on the type of incoming Nrf2-activating compounds, different cysteine residues, such as for example Cys151, Cys273 and Cys288, are altered, translating into specific biological responses.[49] For instance, Cys151 is essential for the formation of a disulfide bond between two Keap1 molecules, with modifications in this residue causing the impairment of the Keap1-Cul3 interaction.[52,53] As a consequence, these binding sites which are crucial for the stability of the Nrf2-Keap1 complex are alkylated or oxidized, causing a conformational change that results in a decline of the proteasomal degradation activity.[20,44,54] Consequently, de novo synthesized Nrf2 can escape degradation, resulting in an increased accumulation of Nrf2, which can translocate towards the nucleus where it forms a dimer with the small musculoaponeurotic fibrosarcoma proteins (sMaf).[20,44] Then, Nrf2 binds to the antioxidant response elements (ARE) that are located in the promotor regions of target genes, thus promoting the transcription of a variety of cytoprotective and detoxifying enzymes.[46] For instance, this includes phase II detoxifying enzymes such as glutathione-S-transferase (GST) and NAD(P)H:quinone oxidoreductase (NQO1).[42] Therefore, the Keap1-Nrf2-ARE pathway serves as a central cellular defence system against OS, promoting cell survival and maintaining intracellular redox homeostasis.[20,21,43]

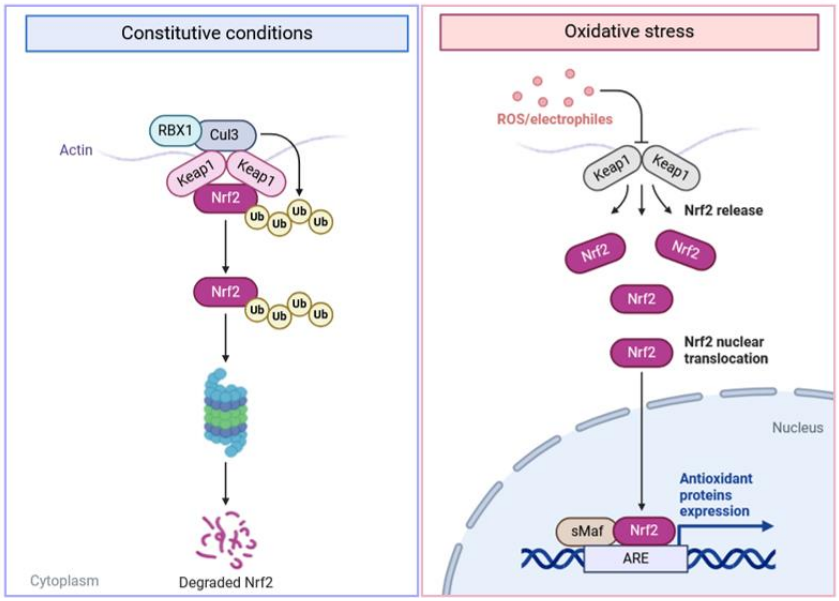

Figure 3: Intracellular signalling mechanism of the Keap1/Nrf2/ARE pathway under constitutive and oxidative stress conditions; created using biorender.com with information compiled from multiple sources.[21,44,50,55]

1.3 Mechanical cues and the tumour microenvironment

Physical stimuli are ubiquitously present in every living cell, being an essential part of communication in biological systems. Cell-cell signalling is essential for adapting to their immediate surroundings, especially at critical stages such as during embryonic development, cell differentiation and regeneration of tissues and organs amongst many others. While chemical signalling mechanisms are involved in the intercommunication between cells and the sensing of their surroundings, a substantial part of these processes is mediated through mechanical cues. This process of transforming physical forces into biochemical signals is called mechanotransduction.[56]

The role of mechanical forces has been emerging as a key point in the formation, progression, metastasis and even therapy resistance of tumour cells.[57] Particularly the tumour microenvironment (TME) seems to have a profound influence on the cancer cell behaviour. It is typically characterized by a highly complex and dynamic mixture of cell types, such as immune- and endothelial cells, as well as cancer-associated fibroblasts.[58] Turbulent surroundings caused by physical forces such as fluid shear stress (FSS) is also a key factor in the TME. As these physical cues can influence the downstream activation of mechanosensitive signalling pathways it is of interest to investigate the role of mechanotransduction to gain insight on cancer cell behaviour.[57]

1.3.1 Mechanotransduction

The transformation of physical stimuli into biochemical signals can be defined as cellular mechanotransduction. It is a crucial part of biological processes in organisms, as mechanical cues are essential for pathophysiological regulation of systems such as wound healing, embryonic development and cancer progression or resistance. [16,57,59] In general, this biological process can be broken down into a sequence three segments, namely mechanotransmission, mechanosensing and mechanosignalling. Firstly, there is a physical force being transmitted onto the cells from their external environment, with some examples for the main mechanical cues that are responsible for cell-matrix interactions in the human body being hydrostatic pressure (HP), tensional- and compressive forces, and fluid shear stress (FSS).[57,60] HP is a commonly present force that is applied by fluids such as blood or air, which can be found in blood vessels or in the lungs. Tensional and compressive forces are the lengthening or shortening of materials through an applied force, which would be the adaptation of muscle fibres during a movement. Shear stress is the frictional force that cells experience when fluid flows on the surface, such as for example when blood is circulated through the vasculature.[56]

Secondly, these initial mechanical signals that are applied on cells are received and converted from a physical cue into one of biochemical nature. These cellular mechanosensors can be divided into different categories, namely the cytoskeleton, in which the actin skeleton plays a major role, mechanosensitive ion channels such as Ca^{2+} channels and cell adhesion molecules (CAM). For example, the tension of the plasma membrane can open the mechanically gated ion channels Piezo1/2 and lead to the influx of extracellular Ca^{2+} into the cells.[60]

Lastly, the mechanosignalling is the cellular response activated because of the incoming extracellular forces.[30] These various biochemical responses can include the induction of gene transcription, cytoskeletal remodelling, as well as alterations in cell behaviour such as in terms of migration or proliferation. Additionally, various signalling pathways seem to be responsive to mechanical stimuli aswell.[61] For example, the RhoA/ROCK pathway is known to be responsive to physical cues, causing downstream effects involved in cytoskeletal remodelling and cell contractility.[57] Interestingly, OS related pathways can also intersect with mechanotransduction. Particularly, Nrf2 was found to be activated through FSS in endothelial cells, leading to the transcription of a variety of ARE encoded genes.[62] This physiological response can be seen in relation to blood vessels being constantly exposed to frictional forces through the laminar flow of blood and need to adapt to changes to maintain homeostasis.[63] Another set of transcription factors known to be activated through mechanical stimuli are the Krüppel-like factors (KLF's). More specifically, KLF2 and KLF4 are well known to respond to FSS in endothelial cells and are involved in the modulation of vascular functions.[64,65] KLF2 will hereby be further elaborated in the following chapter, as it is of particular relevance in the scope of this thesis.

1.3.2 Krüppel-like factors and KLF2

Krüppel-like factors (KLF's) are a group of gene regulatory proteins involved in a variety of cellular processes, such as cell development, apoptosis or proliferation. To date, 17 transcription factors (KLF1-KLF17) have been identified as members of this family, with the defining structural feature being the presence of zinc fingers. While certain KLFs show tissue-specific expression, most of them are widely expressed in the human organism. For example, the expression of KLF1 is mainly reserved to erythroid cells, whereas KLF7 is ubiquitously present in adult tissue. The relevance of the KLF family in the context of cancer research has been increasing, as they are involved in a multitude of regulatory mechanisms, being reported to act as both oncogenes or tumour suppressors.[66] For instance, KLF4 can act as tumour suppressor, as it has been identified to downregulate promoters of related genes in gastric cancer.[67] On the other hand, overexpression of KLF4 was reported to be correlated to a worsened breast cancer prognosis.[68] In endothelial cells, KLF2 and KLF4 play a particularly important role, as a lost expression of these transcription factors was shown to cause aberrant activation of cellular inflammatory responses.[65,69]

While Nrf2 is regarded the master regulator of cellular stress response, KLF2 can be seen the master integrator of endothelial cell functions. This TF is highly expressed in lung tissues, playing a pivotal role in its development of blood vessels.[64] Precisely, knockout of KLF2 in mice caused embryotic lethality due to vascular failure.[70] It was also shown to be involved in other cellular mechanisms, such as adipogenesis or T-cell function.[65] Over two decades ago, the role of KLF2 grew of importance as laminar shear stress was shown to induce the transcription of KLF2 in endothelial cells. It was discovered that KLF2 is upregulated under laminar flow, whereas downregulation was observed under disturbed flow or low shear stress conditions, such as would be present in arterial branch points.[42] In that regard, this shear-responsive TF is involved in the induction and regulator of a

plethora of cellular functions, such as inflammation control, blood vessel development and vascular tone, making it a key focus of vascular biology. The shear-induced activation of KLF2 was reported to reduce the activity of proinflammatory pathways such as NF-κB and AP-1 in endothelial cells. Additionally, upregulation of KLF2 is correlated with the expression of vasoprotective genes such as eNOS (endothelial nitric oxide synthase), which produces nitric oxide to dilate blood vessels.[69]

Interestingly, KLF2 and Nrf2 appear to cooperate in the response to shear stress in endothelial cells, as studies have shown that KLF2 improves the nuclear translocation of Nrf2, playing an important role in the antioxidant activity response of EC.[62] A recent study indicates a crosslink between shear-induced activation of KLF2 and translocation of Nrf2 in endothelial cells.[42] An overexpression of KLF2 in was shown to increase Nrf2 translocation in HUVECS (human umbilical vein endothelial cells).[63] This is of particular interest as it indicates a pathway that is independent on redox signalling in order to activate Nrf2.[64] Illustrated in the following figure (***Fig.4***), the SS/KLF2/Nrf2/ARE pathway can be seen. While the activation of Nrf2 through oxidative stressors has been illustrated in a previous chapter (***Chapter 1.2.2.***), this pathway is of relevance as it indicates an alternate way of upregulating Nrf2 translocation, independent of direct chemical oxidative stimuli. This "hemodynamic defence mechanism" highlights how redox homeostasis can be mediated through flow conditions in endothelial cells.[42]

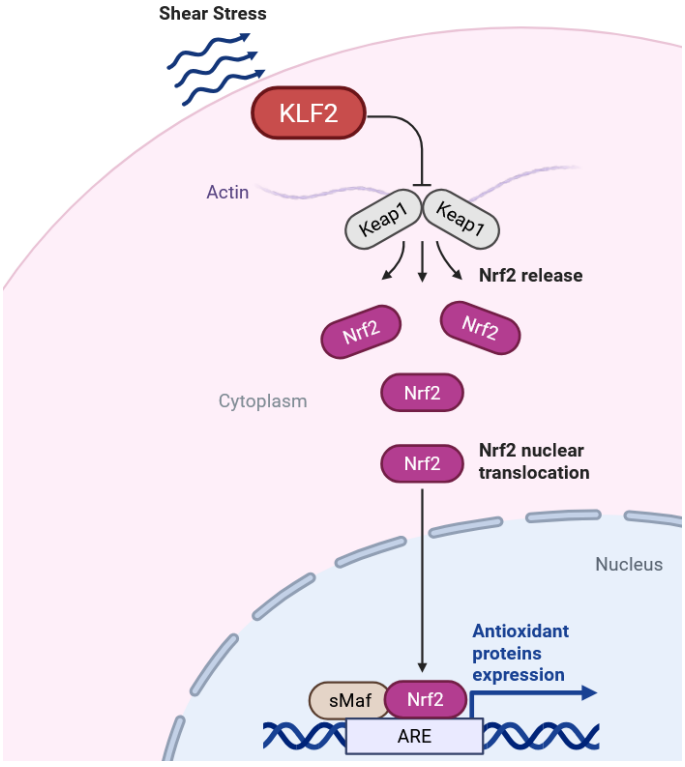

Figure 4: The SS/KLF2/Nrf2/ARE pathway; Created using biorender.com[55]

While the role of KLF2 in endothelial cells is well established, the function of this transcription factor in tumours seems to be more complex. A study comparing cancer cell lines stemming from multiple tissue types revealed that KLF2 is oftentimes downregulated in serous OC cell lines (such as OV177 or SKOV3) when compared to normal tissue[71], whereas the prognosis seems more favourable when expressed.[72] In multiple carcinoma types such as lung or liver cancer, KLF2 is reported to be tumour suppressive, decreasing proliferation and migration, whereas a loss of KLF2 can potentially enhance tumorigenesis.[66,73]

1.4 Role of oxidative stress and mechanical cues in ovarian cancer

Both OS and mechanical forces seem to significantly contribute to OC pathophysiology, oftentimes even in interconnected ways. Ovarian cancer cells typically exist in a state of elevated OS, which influences everything from tumour formation, progression up until drug response.[31] ROS is known to be mutagenic, with elevated levels of ROS being involved in the initiation of tumours. For example, generation of H_2O_2 and hydroxyl radicals produced by the Fenton reaction are correlated to the generation of DNA double-strand breaks in epithelial cells of the fallopian tube.[74] Thus, it is believed that a high OS environment in the ovaries, such as present in chronic inflammation or endometriosis, can lead to malignant cell transformation.[75] The modification of signalling pathways that are involved in the maintenance of redox homeostasis, such as PI3K/AKT/mTOR or Keap1-Nrf2-ARE, have also be reported to be significantly involved in the development of OC. Particularly in regard to the chemoresistance of OC, Nrf2 activation was shown to protect OC cells from oxidative damage and thus reduces the effectiveness of various cytotoxic drugs. Additionally, highly conserved domains in the gene that encodes Keap1 were found to be mutated in various OCs, leading to a lowered suppression of Nrf2. [18] In epithelial ovarian cancer cells, the activation of miRNAs through ROS caused a significant increase of OS and Nrf2 signalling, which was shown to be correlated with promoting tumorigenesis.[76] The expression of Keap1 and Nrf2 was also found to be directly related to the prognosis of OC treatment. Precisely, in a study conducted by Cho et al. they found that patients with an increased expression of Keap1 and thereby lowered translocation of Nrf2 have a better prognosis in terms of survival.[77]

At the same time, the mechanical aspects of the ovarian cancer microenvironment significantly influence disease progression and metastasis. These cells inhabit a dynamic physical environment in the peritoneal cavity, where fluid movements and pressure exert mechanical stress onto them. A common feature in advanced OC is the presence of ascites, affecting around 36.7% of OC patients.[16,78]. This process describes the formation and accumulation of fluids in the abdomen, most likely caused by the obstruction of lymphatic drainage systems, and it can reach volumes up to several litres. The presence of ascites exerts physical forces such as FSS onto surrounding tissues, consequently inducing mechanical stimulation. Additionally, the dynamic flow that is presented through ascites is involved in the transportation of primary tumour cells into other regions of the peritoneal cavity.[23] A major adaptation that is induced by shear stress is the so-called epithelial-to-mesenchymal transition (EMT), a process through which a stationary epithelial cell transforms into a mesenchymal cell that is

capable of being motile.[79] A study conducted by Rizvi et al.[80] suggests that EMT occurs in OC, however the underlying mechanisms orchestrating this transformation have yet to be elucidated. More recently, it was discovered that ovarian cancer cells that were grown under continuous fluid flow developed mesenchymal traits and expressed higher levels of cancer stem cell markers compared to static culture.[81] Nonetheless, it is evident that mechanical cues resulting from FSS and the tumour microenvironment are important precursors of metastasis formation and disease progression of ovarian cancer.[16]

In ovarian cancer, oxidative stress and mechanical forces do not act in isolation, but rather they coexist and potentially reinforce each other. The ascitic fluid, for example, contains numerous inflammatory cells (like macrophages and neutrophils) that generate ROS and secrete cytokines, adding a chemical stress component to the mechanical stress of shear flow. It was reported that ovarian cancer cells preconditioned with ascites showed higher glutathione levels and antioxidant enzyme activities, which made them more capable of surviving subsequent stress and also more adhesive/invasive.[82] Moreover, both OS and mechanical stimuli can converge on common downstream effects like EMT.[80,83] In summary, evidence suggests that OS and mechanical cues seem to be correlated in many terms of OC pathophysiology. Consequently, it is of interest to not only investigate potential chemical pathways that are driven by these chemical and mechanical cues separately, but also try to understand the interplay between them and how this affects the phenotype of OC.

2 Aim of the thesis

The overarching objective of this thesis is to investigate how the exposure of ovarian epithelial cancer (EOC) cells to chemical and mechanical stressors influences the intracellular signalling involved in OS response and how this affects the cell viability. The focus was hereby placed on the Keap1/Nrf2/ARE pathway, particularly on the mechanosensitive TF Nrf2, known as the master regulator of oxidative stress response.[44,62] Another target of investigation was the potential role of the shear-responsive transcription factor KLF2 in this system, which was previously described to prime the translocation of Nrf2.[63,84] To account for the heterogeneous phenotype of OC, two distinct cell lines belonging to type 1 or type 2 classifications were selected, namely the clear cell carcinoma (CCC) SKOV3 and the high-grade serous ovarian cancer (HGSOC)-derived OVCAR3. In general, experimental designs were centred around a 1-hour exposure time to capture the immediate cellular response to the applied stressors.

Overall, the experiments carried out in the scope of this thesis can be categorized into three main objectives.

- The first aim was to establish if the used cell lines are responsive to chemically induced OS via investigation of Nrf2 mediated signalling and if the subsequent activation of antioxidant signalling pathways is taking place. Confirming the functionality of this redox-sensitive signalling system in the deployed cell culture model was hereby essential in providing a baseline for all subsequent experiments.
- Secondly, the next objective was to assess the impact of mechanical cues on the cellular OS response behaviour. Specifically, the impact of fluid shear stress (FSS) on the cellular morphology and the subcellular nuclear translocation of the mechanoresponsive TF Nrf2 and KLF2 was to be investigated. This experiment was designed to provide insights into the mechanosensitive properties of the TF as well as their potential involvement in redox regulation. The investigation of these TF was hereby carried out using immunofluorescence microscopy and image analysis.
- The third and final experiment was to investigate if the combined effects of chemically induced OS and mechanical stress impact the viability and functional adaptability of the EOC cells. It was hypothesized that simultaneous exposure to H_2O_2-mediated OS and FSS may influence cellular adaptability through Nrf2-dependent activation of antioxidant genes. Hence, the viability of the cells under combined physical and chemical stress was to be assessed using the cytotoxicity assays CellTiter Blue (CTB) and Sulforhodamine B (SRB).

Overall, the results obtained in the scope of this thesis should contribute to a deeper understanding of the role of OS and mechanical cues in shaping molecular signalling pathways that potentially promote the aggressive phenotype and chemoresistance of EOC.

3 Materials and methods

In this chapter, an overview of all materials that were used in the scope of this work are presented. This includes chemicals and solutions, antibodies, cell lines, instruments and the software used to obtain and evaluate the data as well as their respective manufacturers. Furthermore, the general experimental procedure will be described. Precisely, this includes the maintenance of the used cell culture models, elaboration of the experimental setups, performance of assays and the statistical evaluation of the obtained data.

3.1 Materials

3.1.1 Consumables

Name	Supplier	Reference ID
µ-Slide 8 Well ibiTreat	Ibidi	80826
Cell culture dish, (ØxH): 60 x 15 mm, 100 x 20 mm	Sarstedt	83.3901, 83.902
Cell culture plate, 12-,24-,96- well, surface: standard, flat bottom	Sarstedt	83.3921, 83.3922, 83.3924
Centrifigation tubes 50ml	Sarstedt	62.547.254
Glass slides (Ø): 10 mm, 18 mm	Marienfeld	0117500, 0117580
Microscope slides	Epredia	AG00000112E01MNZ10
Neubauer counting chamber	Marienfeld	640110
Pipette tips 10, 200, 1000 µl	Sarstedt	70.3010, 70.3030.020, 70.3050.020
SafeSeal reaction tube, 0.5, 1.5, 2 ml, PP, brown	Sarstedt	72.704, 72.690.004, 72.695.500
Serological pipette, 2, 10 ml, sterile	Sarstedt	86.1252.001, 86.1254.001

3.1.2 Instruments

Name	Supplier
Analytical scale: ADB 200-4	Kern
Automated microscope: Lionheart FX	BioTek Instruments
CO_2 incubator: Heracell vios 160i	Thermofisher Scientific
CO_2 incubator: MCO-170AICUV	Phcbi
Inverted microscope: SC50	Olympus
Laminar flow cabinet: CytoFAST elite	Dasit Group
Orbital Shaker: IKA MS 3	Thermofisher Scientific
Plate reader: Agilent Synergy H1	BioTek Instruments
Rocking shaker: SK-R1807-S	DLAB
Vortex mixer: VF2	IKA

3.1.3 Solutions and reagents

Name	Supplier	Reference ID	Additional information
1% acetic acid	Thermofisher Scientific	1733740	diluted in H_2O
Blocking Solution			2% DS in PBS-A
CellTiter-Blue® 10x concentrate	Promega Corporation	G8081	
Donkey serum (DS)	Sigma Aldrich	D9663-10ML	
Dulbecco's Modified Eagle Medium (1X)	Gibco	21063-029	
EDTA	ROTH	1E23.1	
Ethanol (96%) for Fixing	ROTH	P075.1	
Fetal bovine serum (FBS)	Gibco	A525701	
Hydrogenperoxide (30%)	ROTH	8070.2	
Insulin-transferrin-Selenium (ITS)	Gibco	41400045	
McCoy's 5A Medium	Gibco	22330-021	
PBS	Thermofisher Scientific	9150.1	
PBS/EDTA			270 µL (0.5 M EDTA) / 50 mL PBS
PBS-A	ROTH	P029.2, 4984.2, 6781.3, 3904.2	16g NaCl, 4.4g Na_2HPO_4, 0.4g KCl, 0.4g KH_2PO_4 dissolved in 1L Milli-Q H_2O, pH 7.2
PBS-A Glycine			0.35 g /50 mL PBS-A
Penicillin/Streptomycin (P/S)	Gibco	15140122	
Permeabilization buffer			0.2% TTX in PBS-A
Phalloidin-488 Oregon green	Invitrogen	2738348	
ROTI Histofix 4% Formaldehyde	ROTH	344359260	
ROTI®Mount FluorCare DAPI	ROTH	HP20.1	
RPMI Medium 1640 (1x)	Gibco	21875-034	
Sulforhodamine B solution			0.4% (w/v) sulforhodamineB (SRB)
Tris-Base	ROTH	4855.1	
TritonX-100 (TTX)	ROTH	270298309	
Trypan Blue	Sigma Aldrich	T8154	
Trypsin (10x)	Gibco	15400-054	Diluted in PBS
Washing buffer			0.05% TTX in PBS-A

3.1.4 Antibodies, Treatment and Cell lines

	Name	Supplier	Reference ID
Antibodies	Nrf2 antibody	Santa Cruz Biotechnology	ab62352
	KLF2 monoclonal antibody OTI3A10	Invitrogen	MAS-26827
	Alexa Fluor 647 donkey anti-mouse IgG	Invitrogen	AB_162542
	Alexa Fluor 647 donkey anti-rabbit IgG	Invitrogen	AB_2536183
Cell lines	SKOV3 Human ovarian cancer cell line	ATCC	HTB-77
	OVCAR3 Human ovarian cancer cell line	Sigma Aldrich	HTB-161

3.1.5 Software

Name	Supplier
Gen5™ Version 3.08	BioTek Instruments
Microsoft® Excel® (Microsoft Office 365)	Microsoft Corporation
Origin Pro® 2025	OriginLab Corporation

3.2 Cell culture

In this section, the general work routine for cell cultivation and maintenance is described. This includes a description of the cell lines used for the project, the general passaging procedure and counting of cells for experimental usage.

3.2.1 SKOV3 cell line

The ovarian epithelial adenocarcinoma cell line SKOV3 was established from the ascites of a serous cystadenocarcinoma of a 64-year-old Caucasian woman. Regarding their classification, they belong to the subgroup of clear cell carcinomas (CCC).[53] The adherent cells have an oval or elongated morphology and predominantly grow in a monolayer, as can be seen in the following figure (***Fig.5***). This cell line was shown to exhibit resistance to several cytotoxic drugs as well as tumour necrosis factor.[85]

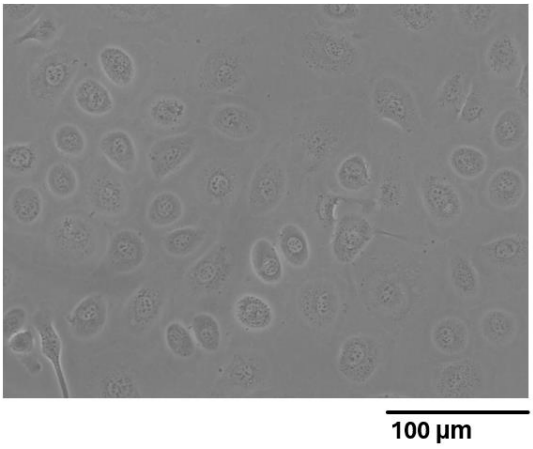

Figure 5: SKOV3 cells; Image taken with Olympus SC50 (20x magnification)

3.2.2 OVCAR3 cell line

The second cell line used in the scope of this thesis is OVCAR3, which are epithelial ovarian cancer cells isolated from a progressive adenocarcinoma in the 1980s. They are classified as HGSOC and the cells predominantly grow in colonies, as can be seen in the following figure (***Fig.6***).[53] Additionally, these cells also show a high resistance towards commonly used chemotherapeutics such as Cisplatin and Adriamycin as well as aggressive growth patterns.[86]

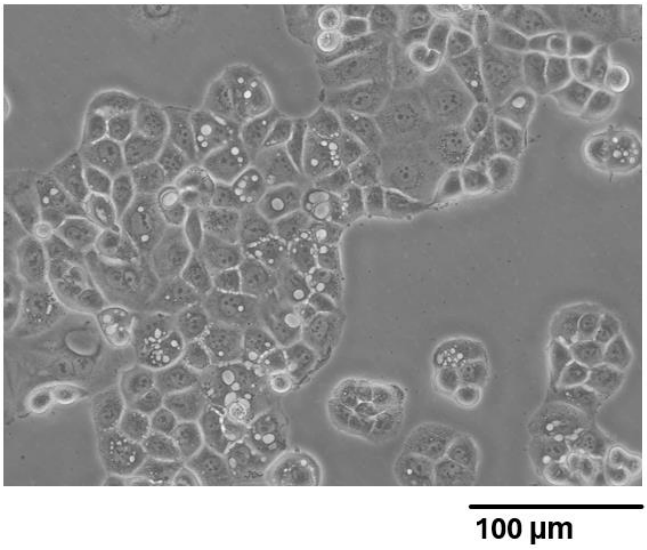

Figure 6: OVCAR3 cells; Image taken with Olympus SC50 (20x magnification)

3.2.3 Maintenance of cell lines

Both cell lines were maintained in 60 mm/100 mm petri dishes and cultured in a humidified incubator under the conditions of 37 °C and 5% CO_2 . For SKOV3, the growth medium comprised of McCoy's 5A Medium, 10% Fetal Bovine Serum (FBS) and 1% Penicillin-Streptomycin (P/S). The cell culture medium for OVCAR3 cells was made up of RPMI 1640 Medium, 20% FBS, 1% insulin-transferrin-selenite (ITS) and 1% P/S. Both media include phenol red as a visual pH indicator, as high concentrations of metabolic products or contaminations usually cause a change in the pH. Additionally, the role of FBS, and in the case of OVCAR3 also ITS, was to promote cell growth and P/S to avoid any potential contaminations from proliferating.

3.2.4 Passaging the cells

To avoid contaminations, the entire workflow was performed in a laminar flow cabinet under sterile conditions. All used solutions were pre-warmed to 37 °C as a decrease in the temperature would be unfavourable for the viability of the cells.

The medium inside the petri dishes was aspirated and 1.5/2 ml of a phosphate buffered saline solution (PBS) containing ethylenediaminetetraacetic acid (EDTA) were added to remove dead cell particles and other debris. The purpose of EDTA was particularly to aid in the detachment of SKOV3 cells as they tend to be more adherent

to the dish surface. The solution was subsequently removed, and 1/1.5 ml of trypsin were pipetted onto the cells to detach them from the bottom of the dish. It was swirled around evenly to cover the surface and then put into the incubator for 5 minutes to let the enzyme work more efficiently. Once the cells were detaching, 3/5 ml of the respective medium were added to quench the activity of trypsin. The suspension was thoroughly mixed and then transferred into a 10 ml tube. A small aliquot of 20 µl was taken out and combined with 80 µl Trypan blue solution to create a 1:5 dilution for the cell counting.

To continue the growth, 220k/500k SKOV3 cells or 500k/1.000k OVCAR3 cells were added to separate small/large petri dishes containing 5/9 ml of the respective medium. The proper volume of cell suspension was added into the dishes, evenly spreading all cells throughout the surface before placing it back into the incubator with the passage number being noted. SKOV3 cells were passaged after reaching a confluency of approximately 90%, which was approximately every two days. For OVCAR3, splitting was done once a confluency of 80-85% was observed, which was mainly after around two to three days of incubation.

3.2.5 Cell counting with a Neubauer chamber

The Neubauer chamber is a thick glass plate that has two counting grids engraved in it, each containing 9 large squares with an area of 1 mm^2. A cover slip was put on top of the counting chambers, creating a gap of 0.1 mm, and 10 µl of the previously prepared Trypan blue cell aliquot were then applied to a chamber. To make sure that no inhomogeneities were present, the aliquot was vortexed shortly before use and pipetted up and down multiple times before adding it to the chambers. The Neubauer chamber was then placed under the microscope and the outer 4 large squares of each chamber were examined. As a result of adding Trypan blue, dead cells appeared dark blue since the dye could get inside the cells through their damaged membranes. On the other hand, viable cells remained clear since their cell membranes are still intact.[87] Only these living cells were considered and manually counted. In the case that the number of counted cells had a difference greater than 10% between the two chambers, the counting was repeated with a newly prepared aliquot. The concentration of the cells in the suspension was then calculated using the following formula (***Eq. 1***).

Equation 1:

$$living\ cell\ number\ \left(\frac{cells}{ml}\right) = \bar{x} \times d\ \times 10000$$

$\bar{x}$ … $aveage\ of\ cells\ for\ all\ counted\ chambers$

d … $dilution\ factor$

With the number of cells per ml of the suspension being determined, slides and plates for following experiments could be seeded.

3.3 Experimental procedures

In this chapter, the main experimental layouts performed in the scope of this master thesis will be elaborated. This includes three main workflows: immunofluorescence staining for KLF2 and Nrf2 after (1) exposure to chemically induced OS and (2) mechanical stimulation through 1 h of FSS, as well as (3) cytotoxicity assays.

3.3.1 Assessment of chemically induced OS on Nrf2 and KLF2

200 µl of a cell suspension containing 25k cells/ml for SKOV3 and 80k cells/ml for OVCAR3 were seeded into each well of an 8-well glass bottom µ-slide and placed in an incubator to grow for 48 h. Following this, the medium was aspirated and cells were treated with 150 µl of medium containing either 0, 50, 100 or 500 µM H_2O_2 for 1 h under static conditions, with each condition being carried out in technical duplicates. Afterwards, the cells were fixed by removing the medium and adding 150 µl of ROTI®Histofix 3.5% formaldehyde solution for 15 minutes in the dark. Each well was then washed using 200 µl PBS-A, followed by 150 µl PBS-A glycine and 200 µl PBS-A again, either being stored in the fridge at 4 °C until further use or immediately stained. The experimental workflow for this procedure has been illustrated in the following figure (***Fig. 7***) for better visual clarity.

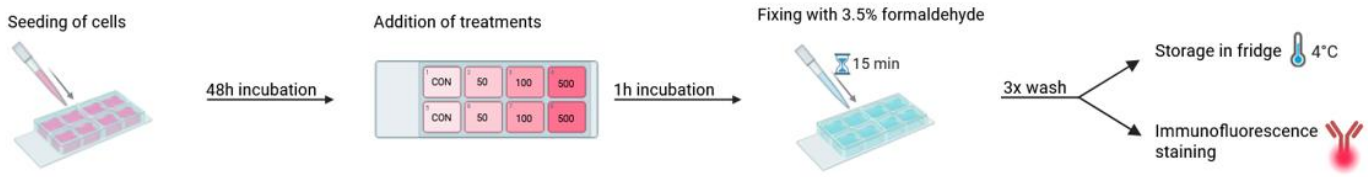

Figure 7: Workflow of the H_2O_2 concentration dependency experiment; Created using BioRender.com

3.3.2 Assessment of mechanical stimulation on Nrf2 and KLF2

To simulate shear stress conditions onto the cells, a previously established protocol from Karasová et al.[88] was taken and adapted. Experiments were carried out in 12-well plates with shaking applied at 300 rpm for 1 h using the IKA MS 3 orbital shaker. This is equivalent to approximately 2 dynes/cm^2 , which was chosen as the range of 0.5-3 dynes/cm^2 was described to induce the stimulation of mechanical cues in ovarian cancer cells.[78,88,89] For each experimental run, 24-well plates with the same treatments were prepared alongside and kept under static conditions.

A cell density of 60k cells/ml for SKOV3 and 140k cells/ml for OVCAR3 were seeded into 12/24-well plates containing microscope glass slides and placed in an incubator to adhere and grow for 48 h. Following this, the cells were then treated with either medium containing 50 µM H_2O_2 or pure culture medium for the control group, with the 12-well plates then being placed on the orbital shaker for 1 h at 300 rpm. In the same manner as described in the previous chapter (***Chapter 3.3.1***), the cells were fixed using 250/500 µl formaldehyde, washed with 500/1000 µl PBS-A and 250/500 µl PBS-A glycine, and placed in the fridge until further use for staining. The layout of the

plates as well as the experimental procedure up until the fixation can be seen in the following figure (***Fig.8***), with each condition being carried out in three technical replicates.

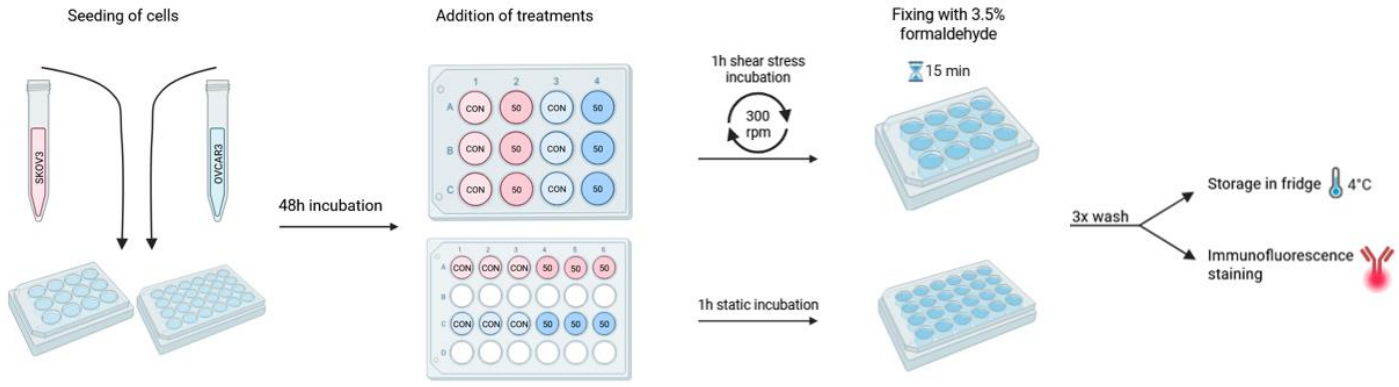

Figure 8: Workflow of the shear stress experiment; Created using BioRender.com

3.3.3 Immunofluorescence Staining:

To determine the effects of physical and chemical stress stimulation cause a modulation of the selected transcription factors KLF2 and Nrf2, immunofluorescence staining was performed. Hereby, the general staining procedure was taken and adapted from a previously established protocol described by Jarolim et al.[90], with the workflow being depicted in the following figure (***Fig.9***).

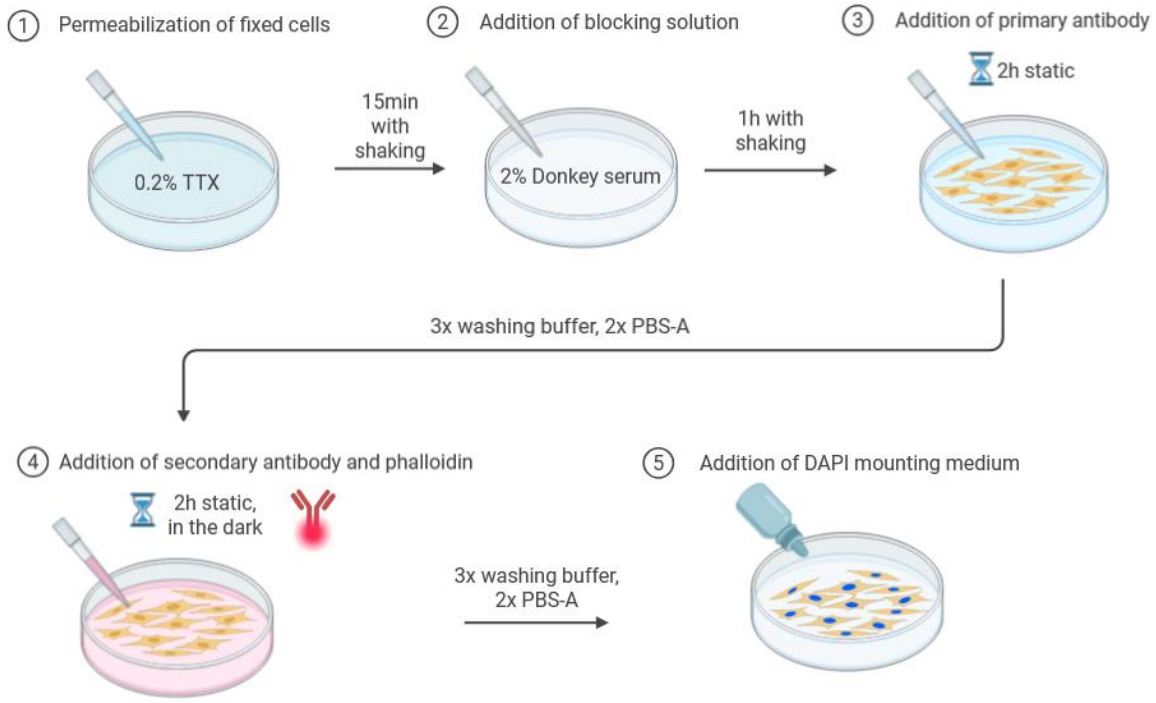

Figure 9: Workflow of the Immunofluorescence staining procedure up until imaging; Created using BioRender.com

Previously fixed 8-well glass bottom µ-slides or 12/24-well plates were taken, and cells were then permeabilized using 150/500/200 µl 0.2% TTX in PBS-A, which removes lipids and damages the cell membrane for the antibodies to get into the cells. This step was done under gentle tilting on a shaker for 15 minutes. Following this step, a blocking solution made up of 2% DS in PBS-A (150/500/200 µl) was added for 1 h to increase the sensitivity of the staining by blocking non-specific binding sites. Primary antibodies for KLF2 and Nrf2 were respectively diluted 1:500 in PBS-A containing 0.25% donkey serum (150/100/50 µl) and added to the now blocked wells for 2 h under static conditions, as to not interfere with the binding of the antibodies to the proteins. Afterwards, each well was washed three times for 10 minutes with washing buffer (150/500/200 µl; 0.05% TTX in PBS-A), followed by washing twice with PBS-A (200/1000/400 µl) for 5 minutes. The slides and plates were then either stored in the fridge or the staining with the secondary antibody was immediately continued. The secondary antibody donkey anti-mouse for KLF2 and donkey anti-rabbit for Nrf2, diluted 1:1000 in 0.25% DS in PBS-A, alongside 1:1000 diluted phalloidin were incubated for 2 h under light exclusion and then washed in the same manner as for the first antibody. Slides were then covered in mounting medium containing DAPI for at least a few hours before imaging. For the shear stress experiment, stained glass discs that were in the 12/24-well plates were inverted onto microscopy glass slides containing DAPI prior to imaging. All experiments were performed in a minimum of three biological replicates.

3.3.4 Cytotoxicity experiments:

To determine if different concentrations of H_2O_2 and mechanical cues impact the cellular adaptability of SKOV3 and OVCAR3 cell lines, cytotoxicity screening was performed through CellTiter™ blue (CTB) cell viability assay coupled with Sulforhodamine B (SRB) assay. The protocol was hereby taken and adapted from Grgic et al.[91] Precisely, 60k cells/ml for SKOV3 and 140k cells/ml for OVCAR3 were seeded into 12- and 96-well plates and left to grow for 24 h. The following day, 12-well plates were shaken for 1 h and 96-well plates were kept under static conditions before incubating the cells with respective media containing 0 (control group), 10, 50, 100 or 500 µM H_2O_2 for 24 h. Each plate hereby contained four technical replicates for control groups and two for each tested condition.

3.3.5 CellTiter™ blue (CTB) cell viability assay:

To determine the cytotoxicity of the tested substances on the deployed cell lines, the CTB cell viability assay was performed. It is a fluorometric method that is based on the metabolic activities which occur in healthy cells, such as the mitochondrial reductase potential. A dark blue redox dye called resazurin is used as an indicator. Through the exposure to viable, metabolically active cells, the substance turns into its reduced form resorufin, which is fluorescent and pink in colour (***Fig.10***). The resulting increase of fluorescence can be measured using a fluorimeter, thus providing information on the number of viable cells present.[92]

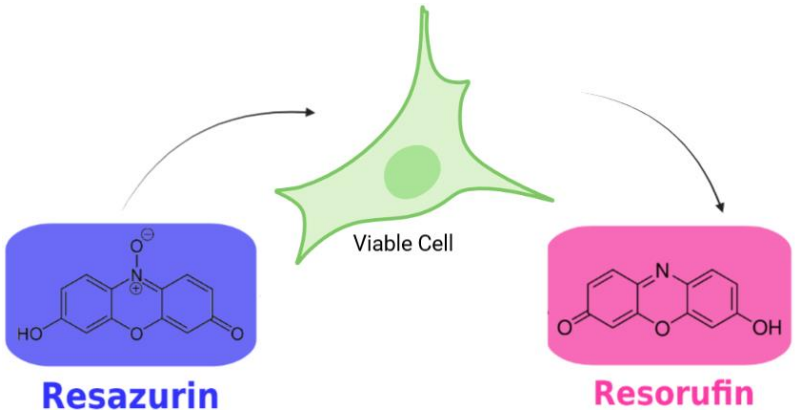

Figure 10*: Schematic depiction of the conversion of resazurin into the fluorescent resorufin through metabolically active cells. Created using BioRender.com*

3.3.5.1 Measuring the cell viability

To measure the cell viability, the CTB buffer was freshly prepared for each biological replicate, with all steps being performed in the dark. To do so, CTB concentrate was diluted in a 1:10 manner with phenol red free Dulbecco's Modified Eagle Medium (DMEM). The medium of every well containing cells was quickly removed and 100 µl of the CTB-buffer were added per well of a 96-well plate or 500 µl per well of a 12-well plate. The plates were then transferred back into the incubator where they were left to react for 2 h. After the incubation time ended, 80 µl of supernatant of each well was transferred into a black 96-well plate, making sure to not create any bubbles. The fluorescence was measured with Synergy H1 Hybrid microplate reader at an excitation wavelength of 560 nm and an emission wavelength of 590 nm. The obtained data was then exported as Excel files for further analysis.

3.3.6 Sulforhodamine B (SRB) Assay

The SRB assay is a method of determining the total protein content of adherent and suspension cells. It is based on the binding properties of Sulforhodamine B (***Fig.11***), a dye belonging to the group of aminoxanthenes, to the basic amino acids of proteins under mildly acidic conditions. The resulting SRB/protein complex can be measured and quantified using a photometer, making it a sensitive method of assessing the cytotoxicity or proliferative effects that treatments or conditions can have on cell cultures.[93]

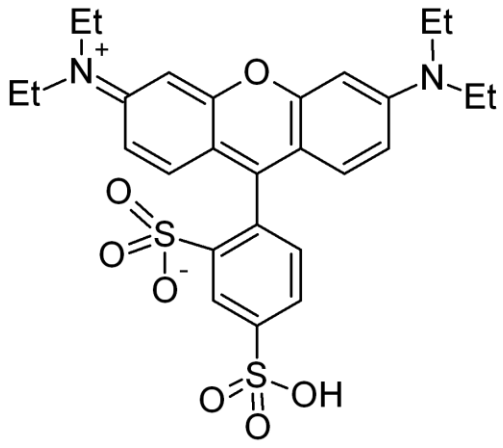

Figure 11: Chemical structure of Sulforhodamine B; Created using ChemDraw

3.3.6.1 Measuring the total protein content

To perform the assay, the 96- and 12-well plates previously used for the CTB assay were fixed with 100/500 µl EtOH (96%) for 15 minutes. This was followed by two washing steps using PBS-A (200/500 µl) and storage of the plates at 4 °C until further use.

To assess the total protein content, the wells containing fixed cells were washed twice with tap water and stored uncovered in a drawer to dry overnight. The following day, 50/250 µl of SRB solution were added to the respective wells of the 96-/12-well plates and left to incubate in the drawer for 1h. Afterwards, the solution was removed, and the wells were washed three times with tap water. Additionally, to make sure that the unbound dye is completely removed, each plate was also washed three times with 1% acetic acid before being placed back into the drawer to dry overnight. To measure the total protein content, 100/500 µl of Tris base were added to dissolve the dye, whereas 100 µl from the 12-well plates were transferred to a 96-well plate. Finally, the absorbance was measured at 570 nm using the Synergy H1 Hybrid microplate reader and the data exported as Excel sheets for further processing.

3.4 Statistical evaluation

3.4.1 Image analysis

Cells were imaged using the Lionheart FX automated microscope with the software being Gen5. For each technical replicate, three images at different positions of the well/glass slide were taken using the DAPI [377/447nm], GFP [469/525nm] and CY5 [628/685nm] channels. The subsequent cellular analysis was performed in the same program by creating a mask for the respective cell lines. To do so, for the nuclear area the primary mask was adjusted with the DAPI channel and for the cytoplasmic area a secondary mask was applied using the GFP channel, which depicts the cytoskeleton of the cell. Calculated cellular areas and intensities were then exported as Excel files, whereas outliers and cells who did not properly fit the mask were excluded.

For image processing and cellular analysis, average intensities of nuclear and cytoplasmic areas per image were calculated in Excel 2025. To do so, the ratio between nuclear and cytoplasmic areas (n/c ratio) were determined for individual cells and averaged per image. Origin Pro 2025 was then used for further data processing as well as for the visualization of obtained results. Significant differences were determined using Student's t-test, with significant differences of $p<0.05$ being indicated with an asterix (*) for comparisons between control and H_2O_2 concentrations and a hashtag (#) between static and shear stress (SS) conditions. (* $p<0.05$, ** $p<0.01$, *** $p<0.001$)

3.4.2 Cytotoxicity assays

For both CTB and SRB, the obtained data was evaluated in Excel 2025, with a minimum of three biological replicates being performed per experiment. For each experiment, the mean value of the four technical replicates of the control group was calculated per respective plate. Every tested condition was then divided by that mean value to determine the test/control (T/C) ratio. For better visual clarity, values were multiplied by 100 to be displayed as percentages and then plotted as bar charts and using OriginPro 2025. Values with a significant difference of $p<0.05$ were determined using one-way ANOVA with Fisher-LSD. Statistically significant values between control groups and H_2O_2 were marked with an asterix (*), whereas differences between static and SS conditions are indicated with a hashtag (#). (* $p<0.05$, ** $p<0.01$, *** $p<0.001$)

4 Results

4.1 Effect of chemically induces OS on cellular morphology

To investigate how chemically induced OS potentially affects the morphology of epithelial ovarian cancer cells, different concentrations of H_2O_2 ranging from 50-500 µM were applied to SKOV3 and OVCAR3 cell lines for 1h in static conditions. In the following figure (***Fig.12***), the effect on the actin cytoskeleton for both cell lines are depicted. For both cell lines, no significant variation in actin signal intensity was observed.

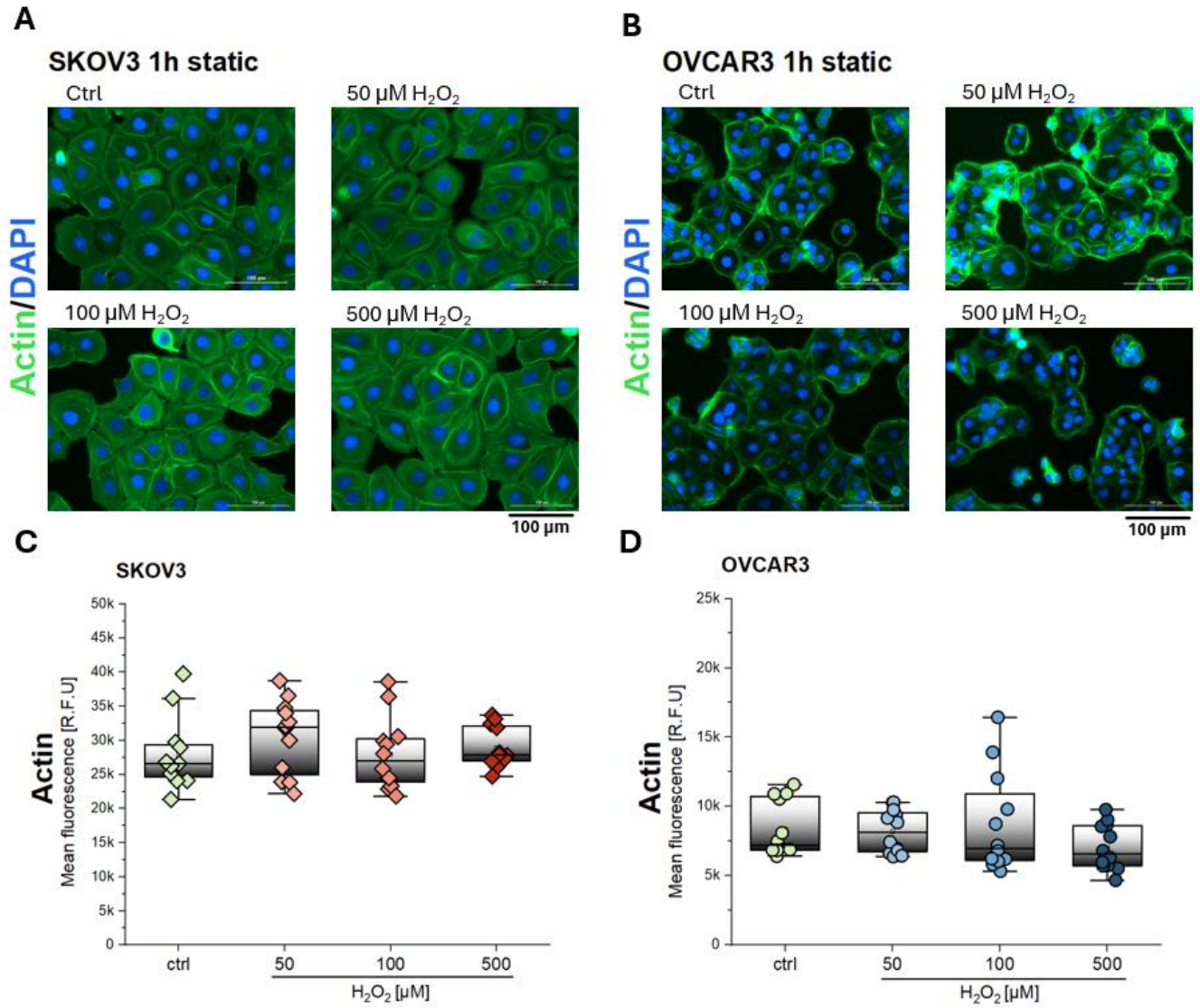

*Figure 12: H_2O_2 concentration dependency in EOCs: Appearance of actin cytoskeleton after incubation with 0-500 µM H_2O_2 for 1 h under static conditions. Displayed are images and quantified mean fluorescence intensity [R.F.U] of actin for SKOV3 (A,C) and OVCAR3 (B,D) cell lines. Cell images (A,B) were acquired using the Lionheart FX automated microscope, 20x magnification, nuclei are displayed in blue and actin cytoskeleton in green. For quantification (C,D), each condition was carried out in technical duplicates and a minimum of three biological replicates per respective cell line. For every sample, three optical fields were randomly chosen for imaging, with the total quantified optical fields per condition being a minimum of n = 18. Statistically significant differences were determined using Students T-test and are indicated with * $p<0.05$, ** $p<0.01$, *** $p<0.001$.*

Similarly, the nuclei of both cell lines were analysed regarding if their morphology is affected by the incubation with H_2O_2. Microscope images and cellular analysis of the nuclear area for SKOV3 and OVCAR3 can be seen in the following figure (***Fig.13***). In both cell lines, no significant changes in nuclear area are observed at all tested concentrations.

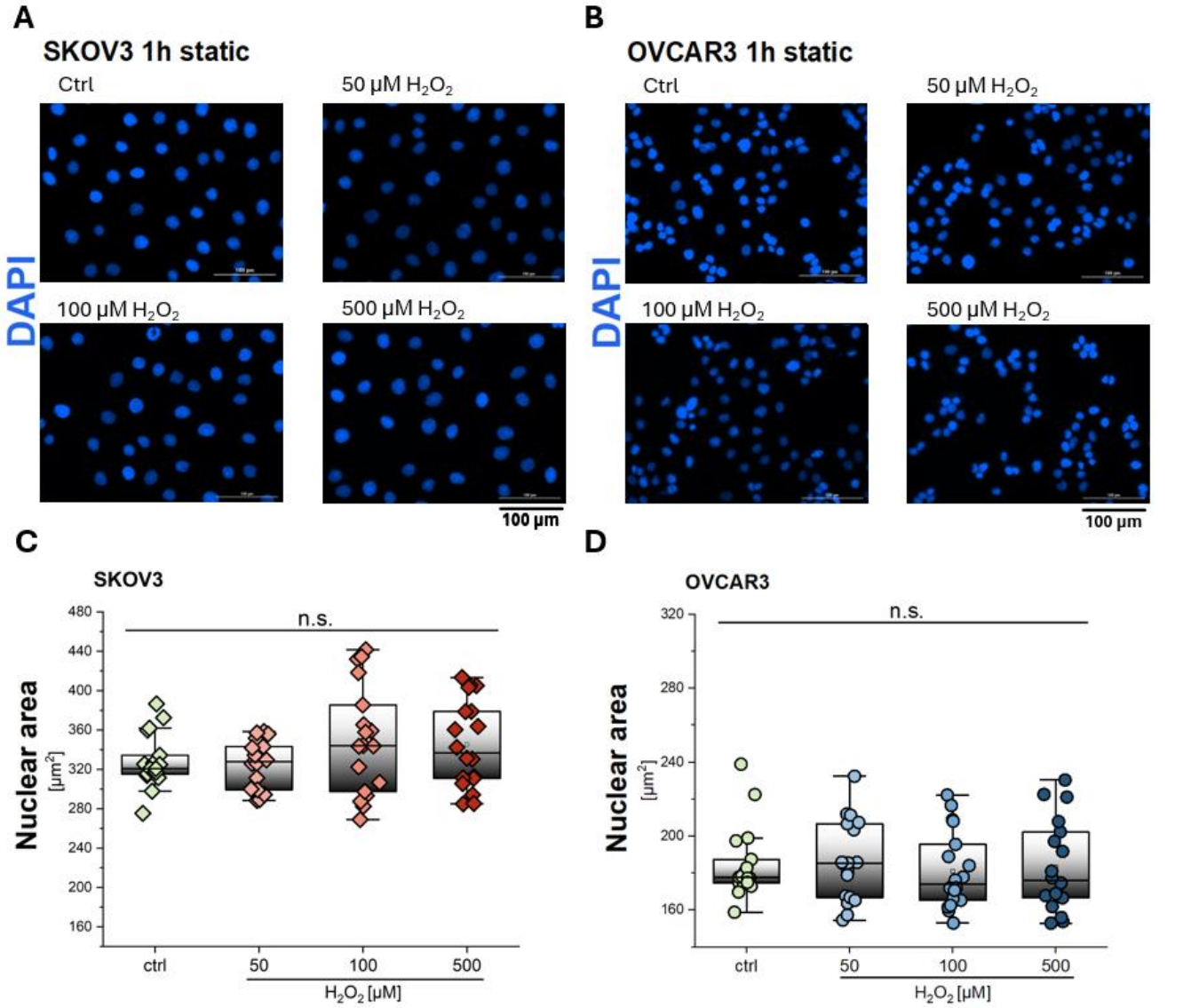

*Figure 13 H_2O_2 concentration dependency in EOCs: Evaluation of the nuclear area after incubation with 0-500 µM H_2O_2 for 1 h under static conditions. Displayed are images and quantified area of nuclei [µm²] for SKOV3 (A,C) and OVCAR3 (B,D) cell lines. Cell images (A,B) were acquired using the Lionheart FX automated microscope, 20x magnification, nuclei are displayed in blue. For quantification of nuclear areas (C,D), each condition was carried out in technical duplicates and a minimum of three biological replicates per respective cell line. For every sample, three optical fields were randomly chosen for imaging, with the total quantified optical fields per condition being a minimum of n = 18. Statistically significant differences were determined using Students T-test and are indicated with * $p<0.05$, ** $p<0.01$, *** $p<0.001$.*

4.2 Response to chemically induced OS on KLF2 and Nrf2

To investigate if signalling pathways involving KLF2 and Nrf2 are responsive to chemically induced OS in SKOV3 and OVCAR3 cell lines, immunofluorescence staining for KLF2 and Nrf2 were performed for incubations with 50-100-500 µM H_2O_2 under static conditions for 1h. Obtained results were quantified as the ratio between nuclear and cytoplasmic signal intensities (n/c ratio), as well as the mean intensities for both cellular regions respectively.

4.2.1 Impact of H_2O_2 concentration dependency on Nrf2

For SKOV3, the quantified results and images of the staining are depicted in the following figure (***Fig.14***).

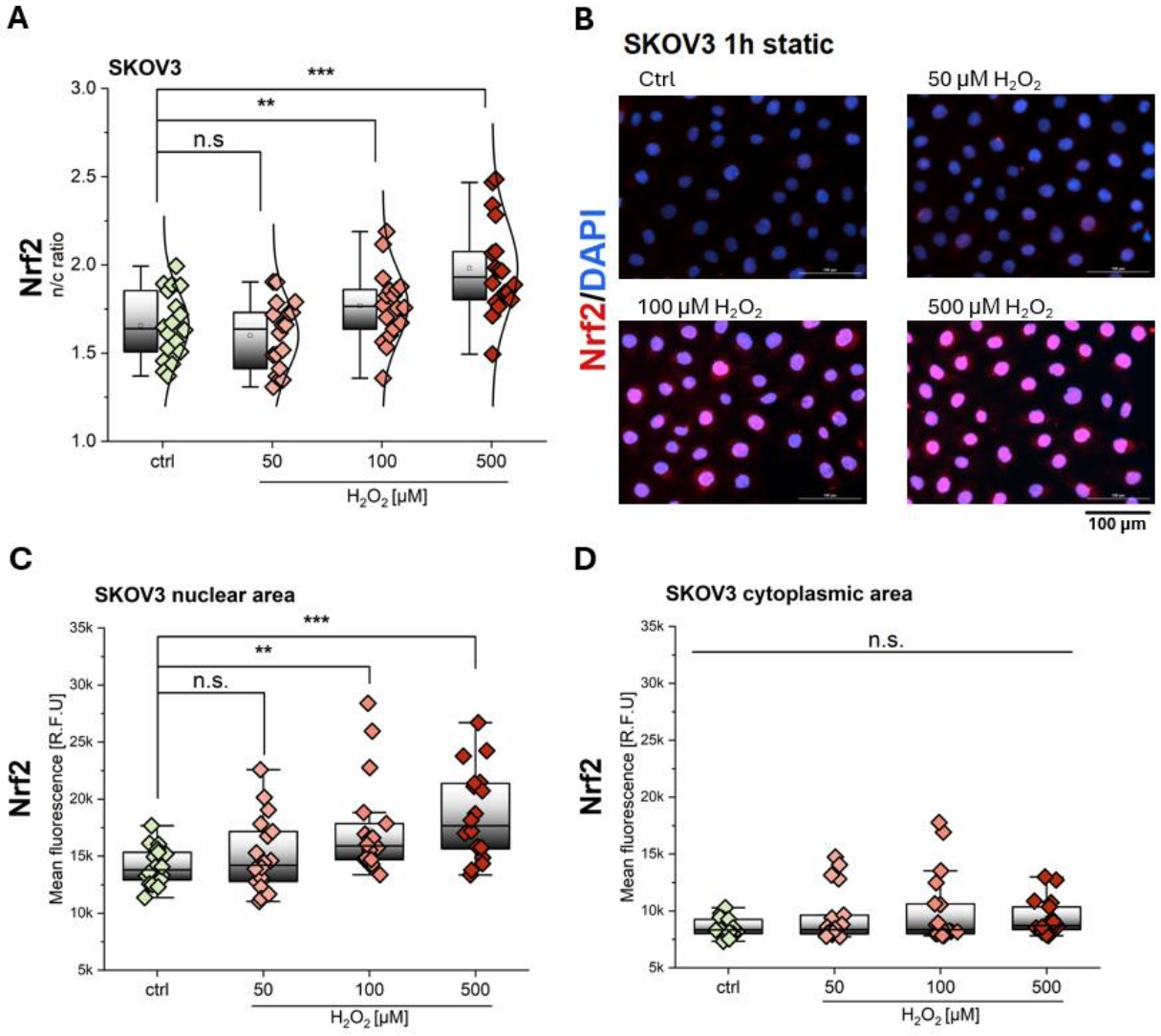

*Figure 14: H_2O_2 concentration dependency in EOCs: Regulation of Nrf2 after incubation of SKOV3 cells with 0-500 µM H_2O_2 for 1 h under static conditions. Displayed are (A) nuclear/cytoplasmic ratio (n/c), (B) images and quantification of (C) nuclear- and (D) cytoplasmic Nrf2 mean fluorescence intensities [R.F.U]. Cell images (B) were acquired using the Lionheart FX automated microscope, 20x magnification, nuclei are displayed in blue. For quantification of nuclear and cytoplasmic areas (C,D), each condition was carried out in technical duplicates and a minimum of three biological replicates. For every sample, three optical fields were randomly chosen for imaging, with the total quantified optical fields per condition being a minimum of n = 18. Statistically significant differences were determined using Students T-test and are indicated with * p<0.05, ** p<0.01, *** p<0.001.*

Looking at the n/c ratio for Nrf2 first (***Fig.14.A***), the results for SKOV3 indicate a significant increase compared to the control group starting at a concentration of 100 µM H_2O_2. This effect is even more evident at the highest concentration of 500 µM H_2O_2, as it is also noticeable in the images of the staining (***Fig.14.B***). It is evident that for SKOV3 the H_2O_2 induced Nrf2 activation mainly takes place in the nuclei, with signal intensities being significantly higher at 100 and 500 µM in the nuclear area (***Fig.14.C***), whereas the cytoplasmic fluorescence intensity remains the same compared to the control group at all tested concentrations (***Fig.14.D***). For OVCAR3, the same trend as for SKOV3 regarding the nuclear activation of Nrf2 through H_2O_2 was also observed in this cell line, as can be seen in the following figure (***Fig.15***).

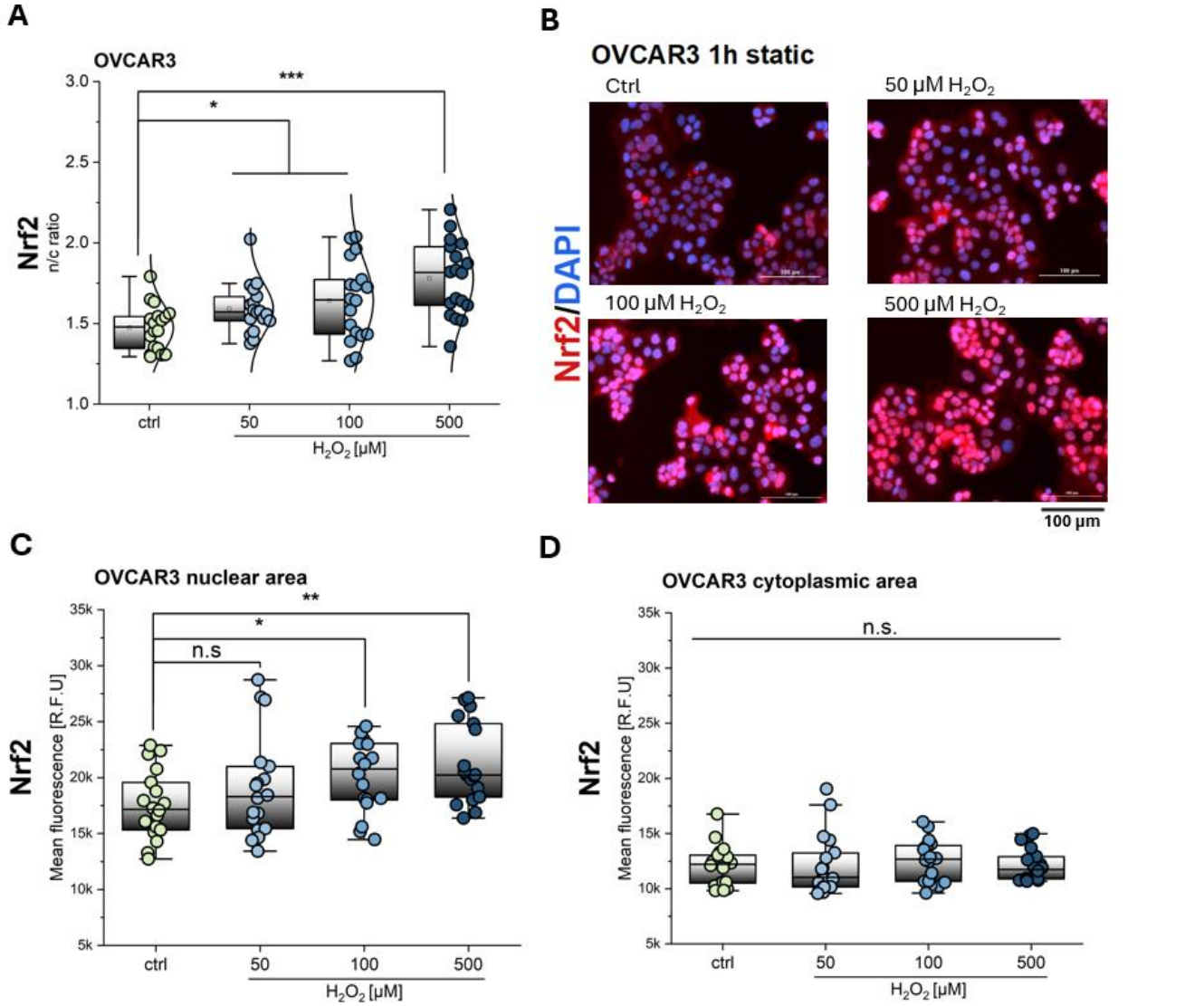

*Figure 15: H_2O_2 concentration dependency in EOCs: Regulation of Nrf2 after incubation of OVCAR3 cells with 0-500 µM H2O2 for 1 h under static conditions. Displayed are (A) nuclear/cytoplasmic ratio (n/c), (B) images and quantification of (C) nuclear- and (D) cytoplasmic Nrf2 mean fluorescence intensities [R.F.U]. Cell images (B) were acquired using the Lionheart FX automated microscope, 20x magnification, nuclei are displayed in blue. For quantification of nuclear and cytoplasmic areas (C,D), each condition was carried out in technical duplicates and a minimum of three biological replicates. For every sample, three optical fields were randomly chosen for imaging, with the total quantified optical fields per condition being a minimum of n = 18. Statistically significant differences were determined using Students T-test and are indicated with * p<0.05, ** p<0.01, *** p<0.001.*

A significant increase in n/c ratio of Nrf2 can already be observed at the lowest tested concentration of 50 µM H_2O_2 (***Fig.15.A***). Similarly to SKOV3 however, an increase in nuclear fluorescence signal was obtained only at 100 µM and 500 µM H_2O_2 in the nuclear area (***Fig.15.C***), whereas the signal in the cytoplasmic area remained unchanged once again (***Fig.15.D***).

4.2.2 Impact of H_2O_2 concentration dependency on KLF2

Regarding KLF2, the obtained results for both cell lines are depicted in the same manner as it was done for Nrf2. Investigating SKOV3 first (***Fig.16***), it is evident that increasing concentrations of H_2O_2 cause a significant concentration dependent decrease of the n/c ratio compared to the control group (***Fig. 16.A***).

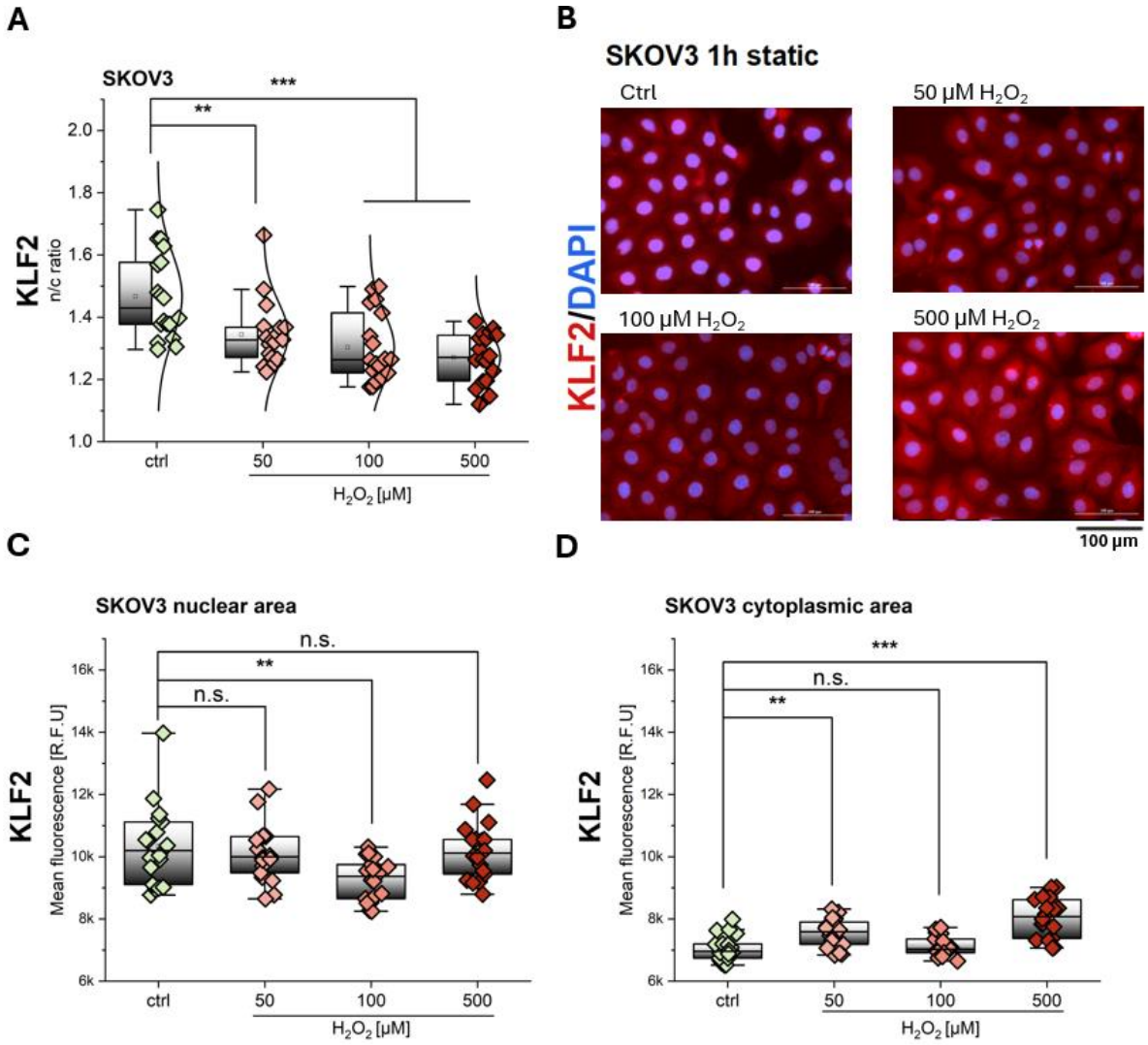

*Figure 16: H_2O_2 concentration dependency in EOCs: Regulation of KLF2 after incubation of SKOV3 cells with 0-500 µM H_2O_2 for 1 h under static conditions. Displayed are (A) nuclear/cytoplasmic ratio (n/c), (B) images and quantification of (C) nuclear- and (D) cytoplasmic KLF2 mean fluorescence intensities [R.F.U]. Cell images (B) were acquired using the Lionheart FX automated microscope, 20x magnification, nuclei are displayed in blue. For quantification of nuclear and cytoplasmic areas (C,D), each condition was carried out in technical duplicates and a minimum of three biological replicates. For every sample, three optical fields were randomly chosen for imaging, with the total quantified optical fields per condition being a minimum of n = 18. Statistically significant differences were determined using Students T-test and are indicated with * $p<0.05$, ** $p<0.01$, *** $p<0.001$.*

While not as prominent at 50 µM H_2O_2, the observed results seem to indicate a signal shift of KLF2 from the nuclear to the cytoplasmic region. Investigating the mean fluorescence intensity for KLF2 in the nuclear area (***Fig.16.C***), it is significantly lowered at 100 µM H_2O_2 compared to the control group, whereas the other concentrations show no significant change. Interestingly, in the cytoplasmic area (***Fig.16.D***), fluorescence of KLF2 seems to be higher at 50 and 500 µM H2O2, whereas it is around the same for 100 µM compared to the control group. Regarding the response of KLF2 to H_2O_2 incubations in the OVCAR3 cell line (***Fig.17***), no significant change in the n/c ratio was found at all tested concentrations (***Fig.17.A***). However, when investigating the mean fluorescence intensities, an increase of KLF2 can be observed in both the nuclear (***Fig.17.C***) and cytoplasmic (***Fig.17.D***) areas when exposed to hydrogen peroxide. Precisely, a significant signal elevation is observed at concentrations of 100 µM and 500 µM H_2O_2.

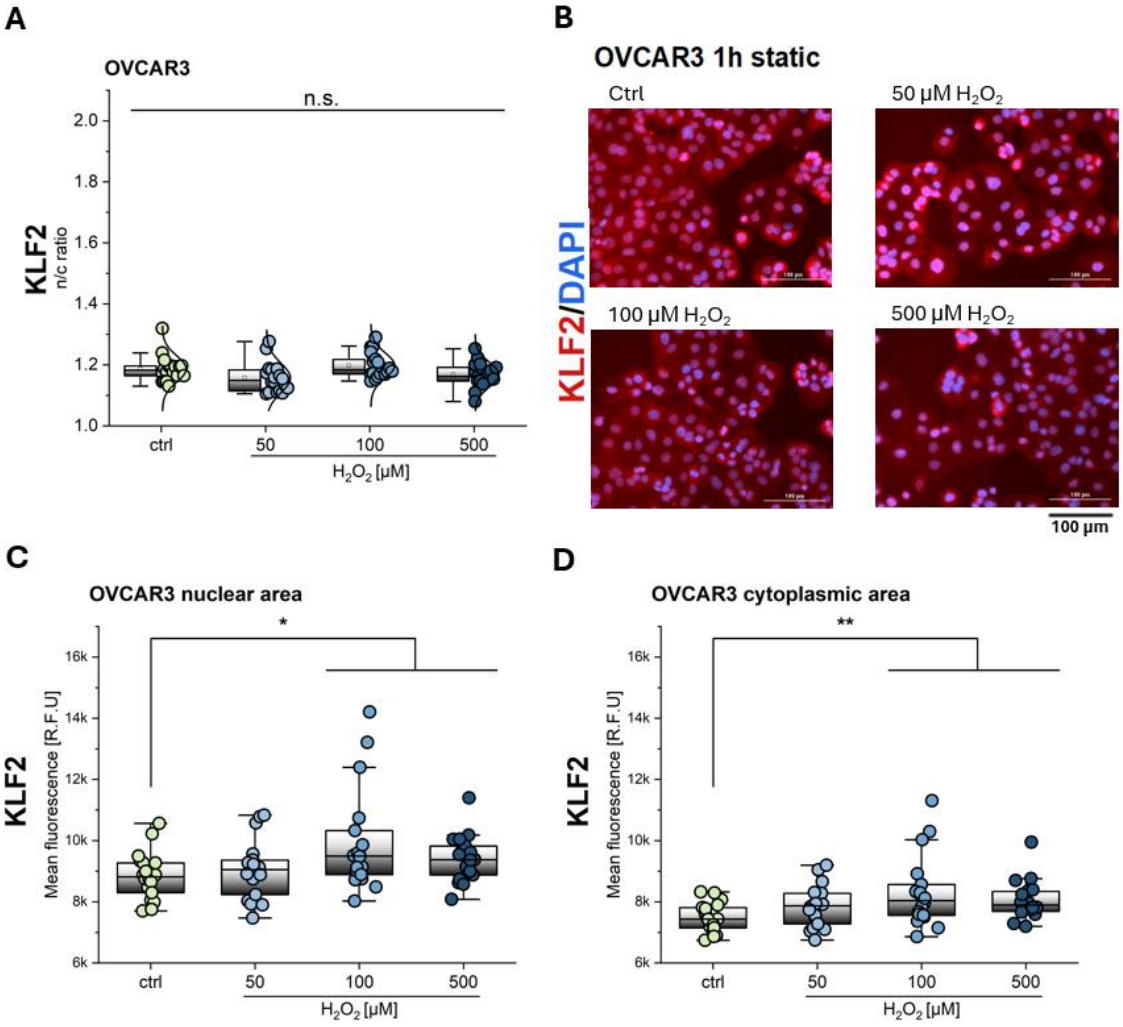

*Figure 17: H_2O_2 concentration dependency in EOCs: Regulation of KLF2 after incubation of OVCAR3 cells with 0-500 µM H_2O_2 for 1 h under static conditions. Displayed are (A) nuclear/cytoplasmic ratio (n/c), (B) images and quantification of (C) nuclear- and (D) cytoplasmic KLF2 mean fluorescence intensities [R.F.U]. Cell images (B) were acquired using the Lionheart FX automated microscope, 20x magnification, nuclei are displayed in blue. For quantification of nuclear and cytoplasmic areas (C,D), each condition was carried out in technical duplicates and a minimum of three biological replicates. For every sample, three optical fields were randomly chosen for imaging, with the total quantified optical fields per condition being a minimum of n = 18. Statistically significant differences were determined using Students T-test and are indicated with * p<0.05, ** p<0.01, *** p<0.001.*

4.3 Influence of mechanical cues on Nrf2 and KLF2

The correlation between shear-induced activation of KLF2 and the translocation of Nrf2 have been observed in endothelial cells.[55] Therefore it was of interest to test if the exposure to shear stress (SS) would alter the cellular response pattern of the presented ovarian cancer cell lines. To investigate this, SKOV3 and OVCAR3 cell lines were exposed to 1 h of SS equivalent to approximately 2 dynes/cm^2 with and without co-incubations of 50 µM H_2O_2. In line with previously presented results, cells were then stained for both mechanosensitive TF respectively and plotted as n/c ratios as well as mean fluorescence intensities of nuclear and cytoplasmic areas.

4.3.1 Impact of SS on Nrf2

The following figure (***Fig.18***) represents the results for the staining of SKOV3 cells after 1h of SS exposure and with or without 50 µM H_2O_2 incubations.

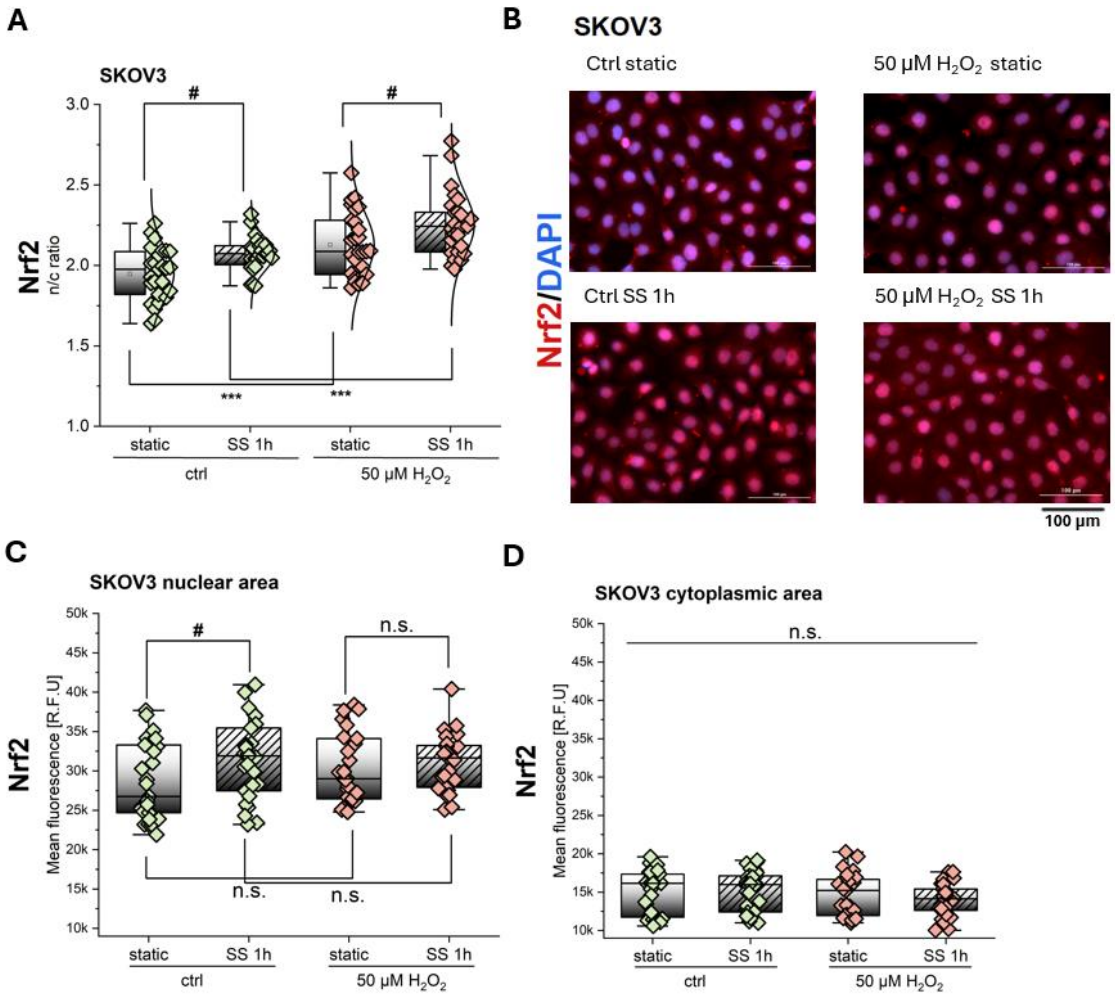

*Figure 18: Shear stress (SS) stimulation in EOCs: Mechanosensitive regulation of Nrf2 after incubation of SKOV3 cells with 0 or 50 µM H_2O_2 for 1 h under static or SS conditions. Displayed are (A) nuclear/cytoplasmic ratio (n/c), (B) images and quantification of (C) nuclear- and (D) cytoplasmic Nrf2 mean fluorescence intensities [R.F.U]. Cell images (B) were acquired using the Lionheart FX automated microscope, 20x magnification, nuclei are displayed in blue. For quantification of nuclear and cytoplasmic areas (C,D), each condition was carried out in technical triplicates and a minimum of three biological replicates. For every sample, three optical fields were randomly chosen for imaging, with the total quantified optical fields per condition being a minimum of n = 27. Statistically significant differences were determined using Students T-test and are indicated with */# p<0.05, **/## p<0.01, ***/### p<0.001.*

Hereby, a significant increase in the ratio (***Fig.18.A***) after 1h SS can be seen for both control and 50 µM H_2O_2 conditions. In line with previously obtained results (see ***Chapter 4.2.1***), the coincubation with 50 µM H_2O_2 seems to further potentiate this effect, leading to an even higher translocation of Nrf2 in the nucleus compared to the control groups. Regarding the mean fluorescence intensities measured, a significant increase in signal was obtained for the control group after 1 h of SS in the nuclear area (***Fig.18.C***). In the cytoplasmic area (***Fig.18.D***), signal intensities remain the same for all tested conditions. For OVCAR3 cells, results were obtained in an analogous fashion as for SKOV3 and are depicted in the figure below (***Fig.19***).

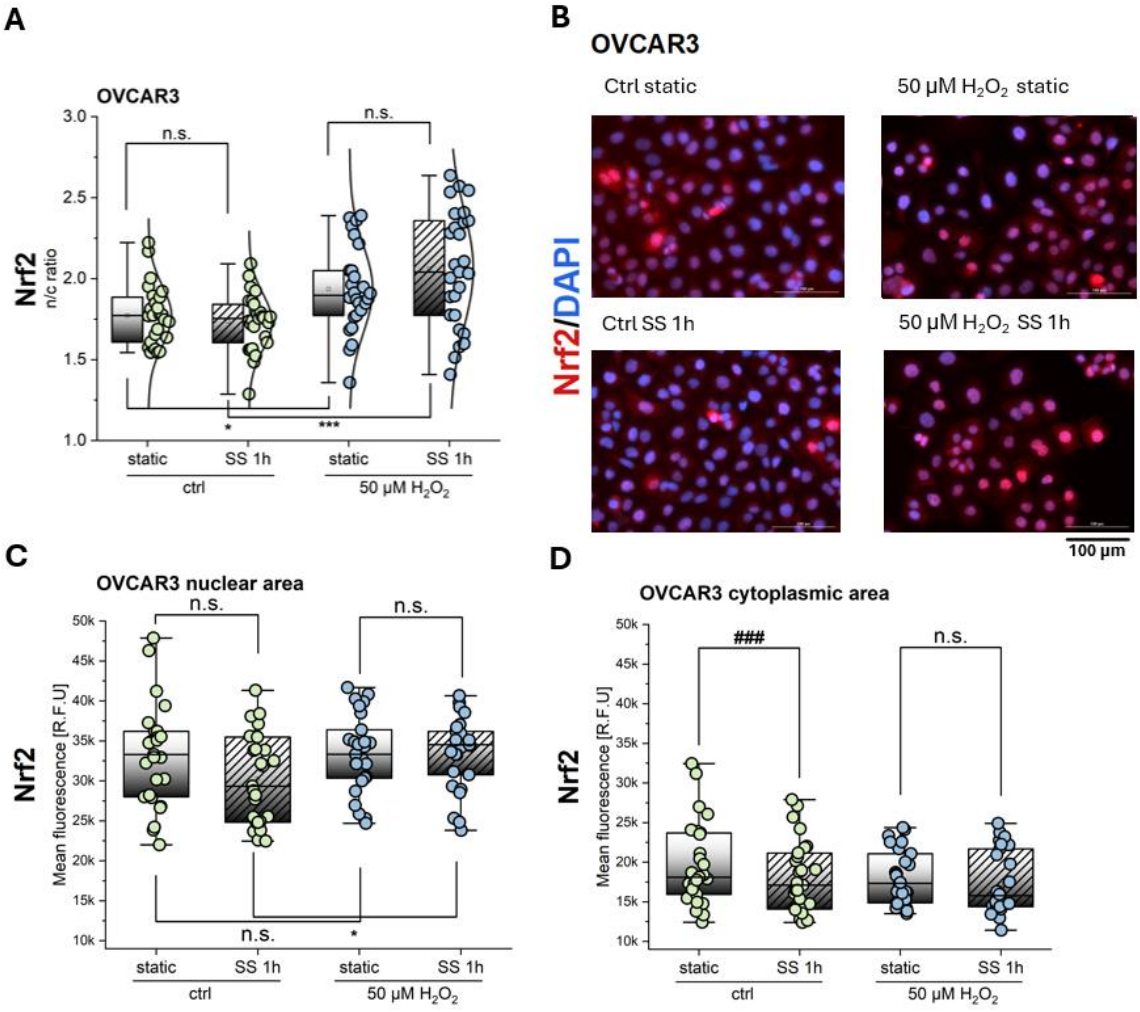

*Figure 19: Shear stress (SS) stimulation in EOCs: Mechanosensitive regulation of Nrf2 after incubation of OVCAR3 cells with 0 or 50 µM H_2O_2 for 1 h under static or SS conditions. Displayed are (A) nuclear/cytoplasmic ratio (n/c), (B) images and quantification of (C) nuclear- and (D) cytoplasmic Nrf2 mean fluorescence intensities [R.F.U]. Cell images (B) were acquired using the Lionheart FX automated microscope, 20x magnification, nuclei are displayed in blue. For quantification of nuclear and cytoplasmic areas (C,D), each condition was carried out in technical triplicates and a minimum of three biological replicates. For every sample, three optical fields were randomly chosen for imaging, with the total quantified optical fields per condition being a minimum of n = 27. Statistically significant differences were determined using Students T-test and are indicated with */# p<0.05, **/## p<0.01, ***/### p<0.001.*

1 h of SS exposure resulted in no significant change in the n/c ratio (***Fig.19.A***) compared to static conditions for both control and 50 µM H_2O_2 groups. However, the n/c ratio broadens with an increase of physical and chemical stressors towards nuclear translocation. Furthermore, while the incubation of 50 µM H_2O_2 under static conditions

only slightly elevates the n/c ratio of Nrf2, this effect seems to be further exacerbated when co-exposed to 1 h of SS. This is evident when looking at the higher statistical significance between the 1h SS control group and the 1h SS with 50 µM H_2O_2 incubations. For the mean fluorescence intensities (***Fig.19.C*** & ***Fig.19.D***), only the control group of 1h SS diverges from the other conditions. A significantly lower signal was observed in the nuclear area (***Fig.19.C***) when compared to 1h of SS with 50 µM H_2O_2 and in the cytoplasmic area (***Fig.19.D***) when evaluated in relation to the static control group.

4.3.2 Impact of SS on KLF2

The results of the SS experiment stained for KLF2 are presented in this chapter, with the obtained data for the SKOV3 cell line being depicted in the next figure (***Fig.20***).

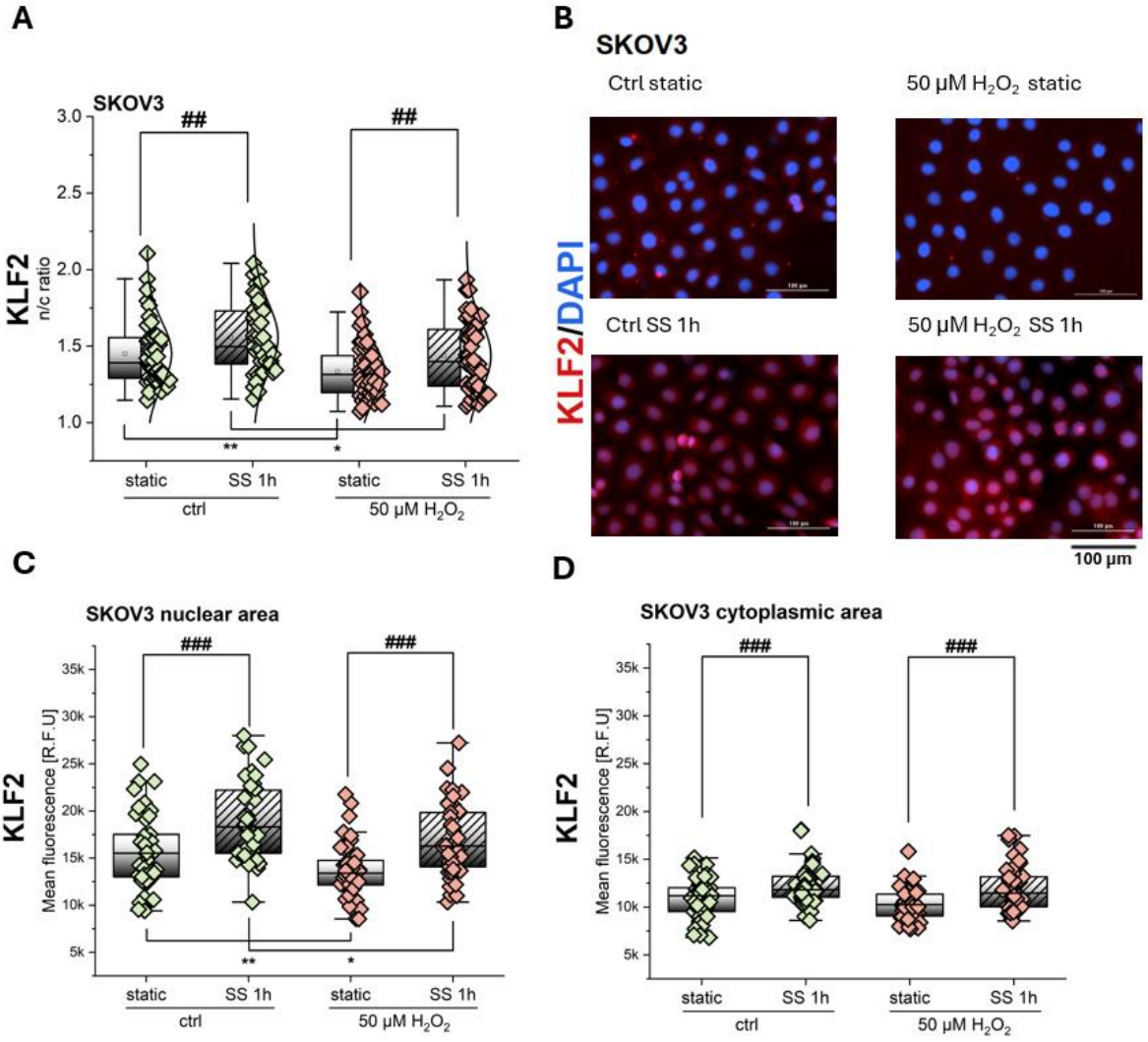

*Figure 20: Shear stress (SS) stimulation in EOCs: Mechanosensitive regulation of KLF2 after incubation of SKOV3 cells with 0 or 50 µM H_2O_2 for 1 h under static or SS conditions. Displayed are (A) nuclear/cytoplasmic ratio (n/c), (B) images and quantification of (C) nuclear- and (D) cytoplasmic KLF2 mean fluorescence intensities [R.F.U]. Cell images (B) were acquired using the Lionheart FX automated microscope, 20x magnification, nuclei are displayed in blue. For quantification of nuclear and cytoplasmic areas (C,D), each condition was carried out in technical triplicates and a minimum of three biological replicates. For every sample, three optical fields were randomly chosen for imaging, with the total quantified optical fields per condition being a minimum of n = 27. Statistically significant differences were determined using Students T-test and are indicated with */# p<0.05, **/## p<0.01, ***/### p<0.001.*

1 h of SS exposure induced a significant increase in n/c ratio (***Fig.20.A***) for both control group and 50 µM H_2O_2. While the distribution of KLF2 towards the cytoplasm when exposed to H_2O_2 under static conditions was already observed (see ***Chapter 4.2.2***), the co-exposure with 1h SS seems to dampen this effect. This is evident when observing the n/c ratio of the control and 50 µM H_2O_2 groups under 1h SS as opposed to under static conditions. Regarding signal intensities, mean fluorescence was significantly increased in both nuclear (***Fig.20.C***) and cytoplasmic areas (***Fig.20.D***). For OVCAR3, the results for the same experiment can be investigated in the following figure (***Fig.21***).

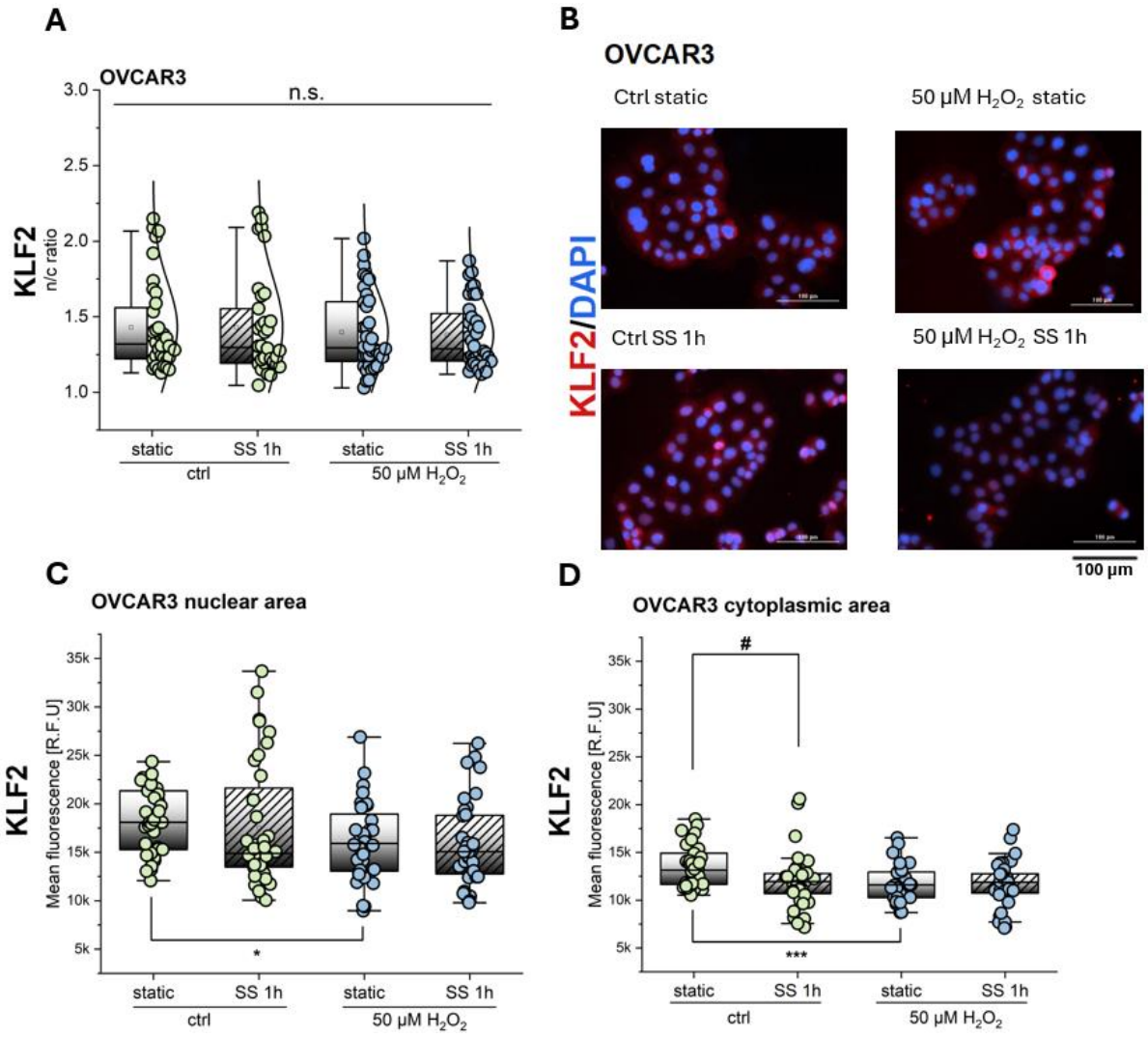

*Figure 21: Shear stress (SS) stimulation in EOCs: Mechanosensitive regulation of KLF2 after incubation of OVCAR3 cells with 0 or 50 µM H_2O_2 for 1 h under static or SS conditions. Displayed are (A) nuclear/cytoplasmic ratio (n/c), (B) images and quantification of (C) nuclear- and (D) cytoplasmic KLF2 mean fluorescence intensities [R.F.U]. Cell images (B) were acquired using the Lionheart FX automated microscope, 20x magnification, nuclei are displayed in blue. For quantification of nuclear and cytoplasmic areas (C,D), each condition was carried out in technical triplicates and a minimum of three biological replicates. For every sample, three optical fields were randomly chosen for imaging, with the total quantified optical fields per condition being a minimum of n = 27. Statistically significant differences were determined using Students T-test and are indicated with */# p<0.05, **/## p<0.01, ***/### p<0.001.*

Contrary to SKOV3, this cell line shows no significant changes in the n/c ratio (***Fig.22.A***), which is also evident when looking at the microscopy images (***Fig.22.B***). Slight differences in signal intensities can be observed when

comparing the control and 50 µM H_2O_2 groups under static conditions in the nuclear (***Fig.21.C***) and cytoplasmic areas (D). These measurements did not align to previous results (see ***Fig.17***), whose cause requires further investigation.

4.4 Effect on cytotoxicity (CTB and SRB)

Finally, it was of interest to elucidate if shear induced mechanical stimulation in combination with H_2O_2 exposure impacts the cell survival. Therefore, the cell viability and total protein content were assessed using the CTB and SRB assays respectively. SKOV3 and OVCAR3 cells were either kept under static conditions or exposed to 1h SS before incubating with a concentration range of 10-50-100-500 µM H_2O_2 for 24 h, after which the assays were performed.

4.4.1 CTB results

The obtained results of the CTB assay for both cell lines can be seen in the following figure (***Fig.22***), with the control groups being set to 100% to better elucidate potential cytotoxic or proliferative effects.

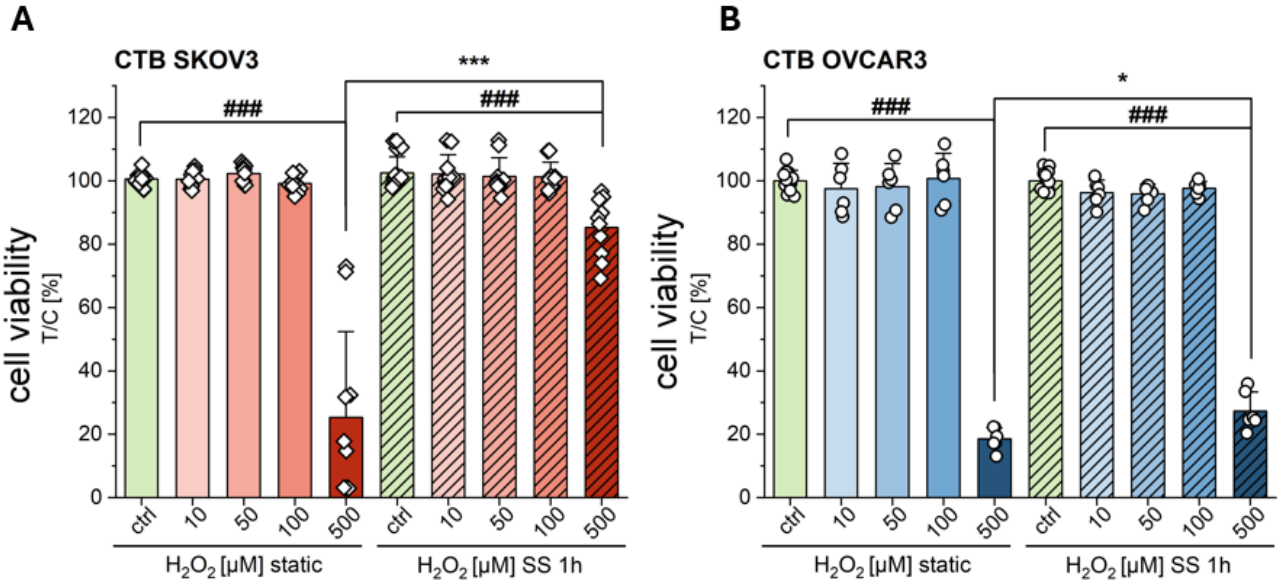

*Figure 22: Combinatory effects of chemically and mechanically induced OS on cell viability of EOC: Results of the CellTiter Blue (CTB) cell viability assay for (A) SKOV3 and (B) OVCAR3 cells after preconditioning with or without 1 h SS, followed by incubation with 0-10-50-100-500 µM H_2O_2 for 24 h under static conditions. Displayed as bar charts is the cell viability as treatment over control (T/C) ratios [%], with the control groups (ctrl) being set to 100%. Data was obtained using the Synergy H1 Hybrid microplate reader. Each condition was carried out in technical duplicates and a minimum of three biological replicates. Significant differences were determined using one-way ANOVA and are indicated with */# $p<0.05$, **/## $p<0.01$, ***/### $p<0.001$.*

Examining SKOV3 first (***Fig.23.A***), cytotoxic effects started taking place at the highest concentration of 500 µM H_2O_2, with the viability being reduced to around 20% compared to controls. Remarkably, 1 h SS pre-exposure at the same concentration significantly reduced the cytotoxic potential of the H_2O_2, bringing it up to approximately 85%. For all other tested concentrations, no variances between static and 1 h SS conditions were observed. While not as prominent compared to SKOV3, the results of OVCAR3 (***Fig.23.B***) follow a similar response pattern regarding the cell viability. The only cytotoxic effect started taking place at a concentration of 500 µM H_2O_2, at

which the viability is at approximately 18% for static conditions. A significant difference is also observable between static and 1 h SS conditions in this cell line, with the cytotoxic effect being slightly reduced, and cell viability reaching 25% when pre-exposed to 1h SS before the chemical treatment.

4.4.2 SRB results

The results of the SRB assay for both cell lines have been compiled in the following figure (***Fig.23***). The data was displayed as the total cell protein amount and expressed as T/C taking the control group as reference (set to 100%). Focussing on the results of SKOV3 first (***Fig.23.A***), cell protein mass seems to not change significantly under both static and 1 h SS conditions except for the highest concentration of 500 µM H_2O_2. In alignment with the CTB results, the total protein amount is significantly decreased under static conditions, whereas the same effect is present yet less prominent under 1 h SS conditions.

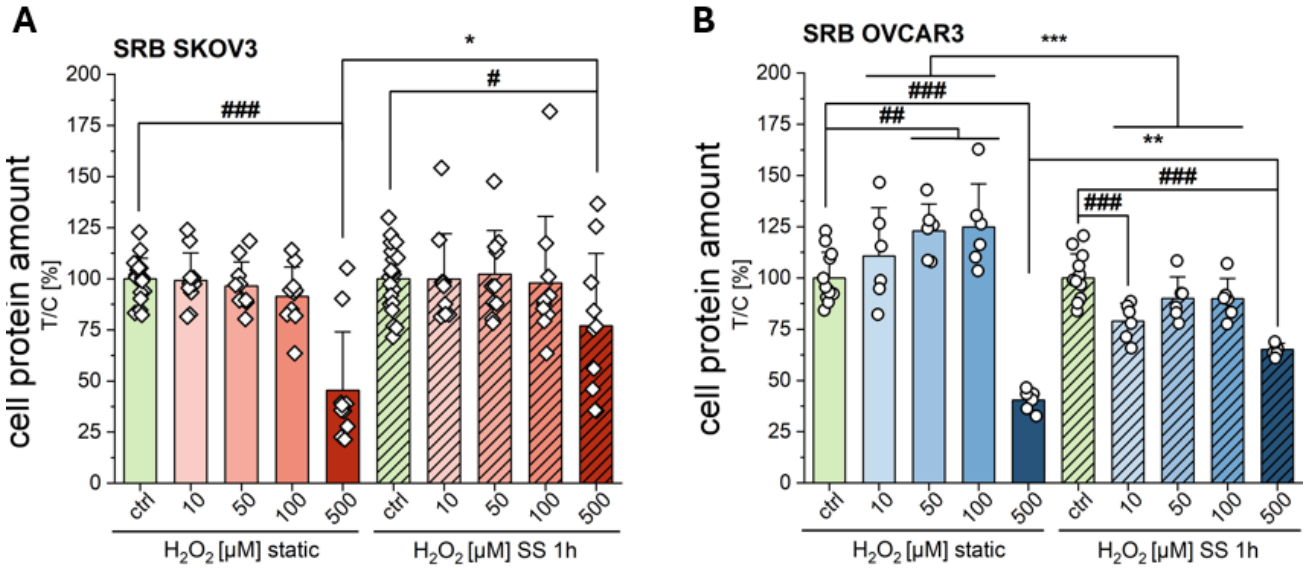

*Figure 23: Combinatory effects of chemically and mechanically induced OS on cell viability of EOC: Results of the Sulforhodamine B (SRB) cytotoxicity assay for (A) SKOV3 and (B) OVCAR3 cells after preconditioning with or without 1 h SS, followed by incubation with 0-10-50-100-500 µM H_2O_2 for 24 h under static conditions. Displayed as bar charts is the total cell protein amount as treatment over control (T/C) ratios [%], with the control groups (ctrl) being set to 100%. Data was obtained using the Synergy H1 Hybrid microplate reader. Each condition was carried out in technical duplicates and a minimum of three biological replicates. Significant differences were determined using one-way ANOVA and are indicated with */# p<0.05, **/## p<0.01, ***/### p<0.001.*

Regarding the SRB analysis of OVCAR3 (***Fig.24.B***), obtained results indicate that under static conditions, lower concentrations of H_2O_2 (50 µM and 100 µM) caused a significant increase in total protein mass compared to the control group. At the highest concentration of 500 µM H_2O_2, a significant reduction of the cell protein amount to around 40% was observed. Under 1 h SS exposure, OVCAR3 cells showed no significant increase in the cell protein amount at all tested concentrations. However, at 10 and 500 µM H_2O_2, a significant decrease compared to the control was observed. Comparing the static and 1h SS results, it is evident that at lower concentrations (10-100 µM), total cell protein amount is significantly lowered under 1 h SS conditions. Contrary, at 500 µM the protein mass is elevated when preconditioned with 1 h SS compared to the results obtained in static conditions.

4.5 Discussion:

OC is a very heterogeneous disease and the resistance to chemotherapeutics is a key driver of poor treatment prognosis.[31,32,94] Elevated levels of OS are a typical characteristic of the ovarian cancer microenvironment[18], and ROS were found to be a key driver in metastatic spread.[83] To withstand high levels of ROS that would be lethal to non-transformed cells, OC cells adapt by boosting their antioxidant defences. The transcription factor Nrf2, known for orchestrating a multitude of intracellular antioxidant responses, has emerged as a key player involved in the aggressiveness and chemoresistance of OC.[43] In addition to chemical cues, ovarian cancer cells are surrounded by a very dynamic environment, with ascites and movements from other organs influencing the microenvironment of these cells. While the involvement of elevated levels of oxidative stress in tumour development, progression and metastasis has been extensively studied, the involvement of fluid shear stress on the redox homeostasis has only gained attention in recent years.[31] In the scope of this thesis, the main objective was to assess how chemically induced OS and physical cues impact two OC cell lines, SKOV3 and OVCAR3, with a specific focus on their morphology, activation of the Nrf2 and KLF2 signalling pathways and the impact on cell viability.

The adaptation of cells to their surrounding environment is a natural response, with a certain level of plasticity being necessary to respond to outward changes. The TME of OC is particularly dynamic, being characterized by various physical and chemical stimuli that can alter the cell morphology and drive them towards becoming metastatic.[58,78,89] The impact of mechanical cues in OC, particularly fluid shear stress, has been previously studied, with the formation of stress fibers as well as changes in the nuclear area being observed.[95] For instance, OVCAR3 cells expressed increased stress fiber formation and actin rearrangement after 3 h of SS exposure.[89] In that regard, it was of interest to see if elevated levels of ROS would also affect the cell morphology in relation to the actin cytoskeleton and nuclear area. Investigating the results of the actin cytoskeleton for SKOV3 (***Fig.12***), the actin signal intensity of the cells seems to remain unaffected by the exposure of H_2O_2. Similarly responding to H_2O_2 as SKOV3, OVCAR3 also show no alterations in actin signal intensities. Additionally, the induction of OS is correlated to enlargements of nuclear areas[96], changes in nuclear area were also investigated. However, as it can be seen in the results for the morphology of the nuclei (***Fig.13***), no significant alterations in the nuclear area were observed for both cell lines at all tested concentrations. These results could be explained by the fact the incubation time with the chemical stressor was set at a 1h time point, making it a rather short exposure time. On the other hand, it could also very well be explained by the fact that H_2O_2 is a naturally occurring signalling molecule in the cells, with the chosen concentrations and incubation times not significantly affecting the cellular behaviour at this level.

The translocation of the transcription factor Nrf2 in response to elevated levels of ROS is a relatively well established pathway.[97] Transcription of antioxidant enzymes encoded in the ARE in response to OS is hereby one

of the main mechanisms which is activated by Nrf2 translocation. [20,41,77] Both SKOV3 and OVCAR3 are known to have a high resistance towards platinum-based chemotherapeutic treatment. In this regard Nrf2 may play a key role, as inhibition of this TF was shown to sensitize SKOV3 cells towards Cisplatin treatment.[98] Additionally, high basal levels of intracellular ROS are suspected to being the reason for increased basal Nrf2 activation in SKOV3 and OVCAR3 cell lines amongst others.[99] Therefore, the next point of investigation was to determine if a chemical stimulation of OS would activate the Keap1/Nrf2/ARE antioxidant defence pathway. To test this, the same concentration range of 50-500 µM H_2O_2 was chosen to mimic mild to more elevated levels of OS[32] in the two cell lines. Indeed, as can be observed in (***Fig.14*** & ***Fig.15***), a concentration-dependent increase of Nrf2 signal as well as translocation towards the nucleus was observed in both SKOV3 and OVCAR3 cell lines after 1h of H_2O_2 exposure. Hereby, it was established that the used cell lines are responsive to ROS as implied by the Nrf2 upregulation and translocation, which provided a fundament for the subsequent experiments that were performed.

The downregulation of KLF2 seems to be a characteristic in OC, with the expression of this TF being significantly lowered in multiple EOC cell lines (amongst which are SKOV3 and OVCAR3) compared to normal ovarian tissue cells.[71] Therefore, it was of interest to see if the exposure to H_2O_2 induced OS would affect the expression in the two cell lines. Investigating SKOV3 first (***Fig.16***), the overall trend indicates a translocation/accumulation of KLF2 towards the cytoplasm with increasing H_2O_2 concentrations. When considering the fluorescence signals of the nuclear and cytoplasmic area, it is evident that the observed pattern is due to an increased signal intensity in the cytoplasmic area. Hence, rather than an increased translocation, SKOV3 cells seem exert an elevated expression of KLF2 in the cytoplasm. Literature data indicate that elevated ROS levels can increase levels of KLF2: KLF2 mRNA expression was found to be elevated in rat cardiac myocytes after incubation with 200 µM H_2O_2, with the highest mRNA expression compared to controls being determined after 1h of incubation time.[100] While this study was not conducted on ovarian cell lines, it does highlight that there seems to be a correlation between elevated ROS and increase in KLF2 expression. In the case of OVCAR3 cells (***Fig.17***), increased signal intensities are observed at concentrations starting at 100 µM H_2O_2 in both nuclear and cytoplasmic areas, with the overall n/c ratios not altering significantly compared to controls. This indicates that the expression of KLF2 might also be increased through hydrogen peroxide in this cell line.

The TME of ovarian cancer is a unique environment, being a key component in driving cancer formation, progression and metastasis. Two important characteristics are hereby mechanical impacts from fluid shear stress, as well as elevated levels of ROS.[33,58,89] As OS and mechanical cues coexist, it was of interest to investigate if these aspects not only as separate entities, but if they are intertwined in regard to OC pathophysiology. Overall, the obtained results of the first experiment indicate that SKOV3 and OVCAR3 cell lines respond to elevated levels of chemically induced ROS through the upregulation and increased translocation of Nrf2 towards the nucleus, as well as an increase in the expression of KLF2. Building on these findings, the next point of investigation was to

explore if the antioxidative response is also being activated through mechanical cues, as well as to see if there is any potential synergism when combined with chemical stressors.

As both Nrf2 and KLF2 are known to be mechanosensitive, and the SS induced activation of Nrf2 was found to be mediated through priming of KLF2 in endothelial cells[101], immunofluorescence analysis for both TFs was performed. In this regard, the obtained results for the SKOV3 cell line clearly highlight that Nrf2 translocation as well as localization in the nucleus in the nucleus is significantly increased after being exposed to 1h of shear stress (***Fig.18*** & ***Fig.19***). Additionally, co-incubation with 50 µM H_2O_2 was found to further potentiate this effect, suggesting that mechanical cues are involved in the upregulation of this antioxidant master regulator. On the other hand, the OVCAR3 cell line present a different behaviour when exposed to SS conditions regarding Nrf2 translocation. It seems as if the combination of physical and chemical stressors does result in an increased Nrf2 mediated response, albeit through a different mechanism compared to SKOV3.

The involvement of KLF2 as a mechanosensitive transcription factor has been well established in endothelial cells, with its shear induced activation being reported to not only reduce proinflammatory pathways, but also improve antioxidant activity through priming Nrf2.[55,69,101] Therefore, it was of interest to see if KLF2 can mirror the observed elevated translocation patterns of Nrf2 in SKOV3 and OVCAR3 cell lines. In that regard, the obtained results for the SKOV3 cell line (***Fig.20***) indicate that a correlation could be possible. 1h of SS caused significantly higher expression and nuclear translocation of KLF2, following the same pattern as observed for Nrf2 (see ***Fig.18***). Therefore, it could be proposed that both OS and the SS/KLF2-mediated activation of Nrf2 take place in this cell line. In OVCAR3 however, the antioxidant response mechanism seems to be uncoupled regarding KLF2, as no changes in quantification of this TF were observed in this cell line (see ***Fig.21***). Since the combination of SS and ROS did cause increased Nrf2 expression in OVCAR3 cells (see ***Fig.19***), it could be postulated that other pathways that respond to mechanical cues are involved, leading to the downstream upregulation of Nrf2. For example, a recent study found that OS induced downstream activation of Nrf2 is mediated by the mechanoresponsive transcription factor YAP1 (Yes-associated protein 1) in human lens epithelial cells.[102] In the context of OC mechanotransduction, a study conducted by Karasová et al.[88] highlights the YAP/TAZ pathway as major responder to SS, driving metabolic and stemness changes in HGSOC cells. It was found that 1h of fluid SS caused the upregulation of the mechanosensitive TF YAP1 amongst others in OVCAR3 cells.[88] While information regarding the interplay between YAP1 and Nrf2 is scarce, some studies suggest a crosstalk between these two TF.[103,104] Therefore, it could be postulated that in case of OVCAR3 cells such a KLF2 independent pathway is involved in the elevated Nrf2 translocation.

Tying all observed results together, the final point to be elucidated was to see if the increased Nrf2-mediated antioxidant response impacts the survival abilities of tested EOC cell lines. Previous studies concluded that Nrf2 signalling pathways are involved in the OC pathophysiology, being involved in many stages of the cancer

progression as well as chemoresistance.[43] While multiple studies have elucidated that a common mechanism through which OC acquires chemoresistance is through upregulation of Nrf2[105–107], underlying mechanisms have yet to be explored in further detail. Particularly, the role of the TME in that regard has been gaining more attention in recent years, being involved in the metastasis and chemoresistance. Cytotoxicity assessments obtained in the scope of thesis indicate that in the SKOV3 cell line, there could be a potential correlation between SS mediated upregulation of Nrf2 and an increased cell survival capability when cells are challenged by oxidative stress. Upon incubation with 500 µM H_2O_2 the cytotoxic effect is significantly decreased when cells are pre-exposed to 1 h of SS compared to static incubation conditions (see ***Fig.22.A*** & ***Fig 23.A***). The activation of the Nrf2 antioxidant pathway plays a key role in the chemoresistance to platinum-based drugs, showing a higher resistance as well as decreased prognosis of survival compared to patients where this TF is inactivated.[107] Particularly the subtype of clear cell carcinomas (CCC), to which the SKOV3 cell line belongs[53], was shown to have a higher localization of Nrf2 to the nucleus as well as expression.[108] As here obtained results elucidated that Nrf2 upregulation in this cell line is activated through both SS as well as OS itself (***Fig.14*** & ***Fig.18***), this can maybe be seen as a functional adaption mechanism. In that regard, the potential role that KLF2 plays in this system has yet to be elucidated. While some studies suggest a correlation between these two TF[84,101], literature findings correlating the two TFs in OC is scarce. Hence, further experiments would be needed to confirm a connection between shear activated KLF2 in priming the Nrf2 mediated antioxidant response that is observed in presented results.

In this regard, OVCAR3 cells, who have expressed a different translocation pattern of KLF2 and Nrf2, seem to also adapt to mechanical stressors, albeit in a different way. Obtained results for the total cell mass determined through SRB (***Fig.23.B***) indicate that low concentrations of H_2O_2 under static conditions have pro-proliferative effects, whereas this is not the case when exposed to SS. It is established that mild levels of OS mediated through H_2O_2 are correlated to the promotion of tumour growth and proliferation[109], which could explain the observed pattern for OVCAR3 cells under static conditions. However, this pro-proliferative effect is diminished in the combination with 1h SS exposure, bringing the total protein expression down to the control group. As FSS imposes an additional stressor for the cells on top of chemical ROS induction, it could be postulated that the overall total OS experienced for this cell line has reached a level that is too high to exert pro-proliferative effects, yet too low to reach levels of cytotoxicity. Interestingly, when the presence of chemically induced OS is very high (500 µM H_2O_2), 1 h of SS seems to act cytoprotective, showing a decrease in cytotoxicity compared to static conditions. As the expression of Nrf2 was shown to be significantly increased at 50 µM H_2O_2 compared to controls when under SS conditions (***Fig.19***), it would be of interest to see if the functional adaptability of OVCAR3 cells could be explained through different Nrf2-mediated mechanisms.

In conclusion, the findings presented in this thesis emphasize the role of both mechanical and chemical cues, as well as their interconnection, in shaping the phenotype of epithelial ovarian cancer (EOC) cells. The CCC cell line SKOV3 seems to adapt in response to the exposure of FSS and H_2O_2, increasing the cell survival capabilities possibly through functional Nrf2 mediated OS adaptation, with a potential involvement of KLF2 in the signalling of downstream antioxidants. In contrast, the more aggressive HGSOC cell line OVCAR3 was shown to express a different phenotype, highlighting the heterogenicity that is inherent to OC. While there are many possible pathways through which OC cells acquire chemoresistance, results collected in this work make it evident that the TME might play a key role in it, and that the various components (eg. ROS, mechanical stimuli, metabolites, …) should not be investigated as separate entities, but much rather focusing on their interplay. In this regard, the obtained data contribute to a better understanding of how stress-responsive pathways, such as Keap1-Nrf2-ARE, influence and shape OC cell behavior. In a broader sense, these findings can hopefully provide insights for further research to identifying novel therapeutic targets and improving existing intervention strategies.

5 References

(1) Stewart, C.; Ralyea, C.; Lockwood, S. Ovarian Cancer: An Integrated Review. *Semin. Oncol. Nurs.* **2019**, *35* (2), 151–156. https://doi.org/10.1016/j.soncn.2019.02.001.

(2) Pawłowska, A.; Rekowska, A.; Kuryło, W.; Pańczyszyn, A.; Kotarski, J.; Wertel, I. Current Understanding on Why Ovarian Cancer Is Resistant to Immune Checkpoint Inhibitors. *Int. J. Mol. Sci.* **2023**, *24* (13), 10859. https://doi.org/10.3390/ijms241310859.

(3) Liao, Y.; Tu, C.; Song, X.; Cai, L. Case Report: Analysis of BRCA1 and BRCA2 Gene Mutations in a Hereditary Ovarian Cancer Family. *J. Assist. Reprod. Genet.* **2020**, *37* (6), 1489–1495. https://doi.org/10.1007/s10815-020-01783-w.

(4) Tavares, V.; Marques, I. S.; Melo, I. G. D.; Assis, J.; Pereira, D.; Medeiros, R. Paradigm Shift: A Comprehensive Review of Ovarian Cancer Management in an Era of Advancements. *Int. J. Mol. Sci.* **2024**, *25* (3), 1845. https://doi.org/10.3390/ijms25031845.

(5) La Vecchia, C. Ovarian Cancer: Epidemiology and Risk Factors. *Eur. J. Cancer Prev.* **2017**, *26* (1), 55–62. https://doi.org/10.1097/CEJ.0000000000000217.

(6) Hanna, L.; Adams, M. Prevention of Ovarian Cancer. *Best Pract. Res. Clin. Obstet. Gynaecol.* **2006**, *20* (2), 339–362. https://doi.org/10.1016/j.bpobgyn.2005.10.016.

(7) Matulonis, U. A.; Sood, A. K.; Fallowfield, L.; Howitt, B. E.; Sehouli, J.; Karlan, B. Y. Ovarian Cancer. *Nat. Rev. Dis. Primer* **2016**, *2* (1), 16061. https://doi.org/10.1038/nrdp.2016.61.

(8) Committeee on the State of the Science in Ovarian Cancer Research; Board on Health Care Services; Institute of Medicine; National Academies of Sciences, Engineering, and Medicine. *Ovarian Cancers: Evolving Paradigms in Research and Care*; National Academies Press: Washington, D.C., 2016; p 21841. https://doi.org/10.17226/21841.

(9) Torre, L. A.; Trabert, B.; DeSantis, C. E.; Miller, K. D.; Samimi, G.; Runowicz, C. D.; Gaudet, M. M.; Jemal, A.; Siegel, R. L. Ovarian Cancer Statistics, 2018. *CA. Cancer J. Clin.* **2018**, *68* (4), 284–296. https://doi.org/10.3322/caac.21456.

(10) Lheureux, S.; Braunstein, M.; Oza, A. M. Epithelial Ovarian Cancer: Evolution of Management in the Era of Precision Medicine. *CA. Cancer J. Clin.* **2019**, *69* (4), 280–304. https://doi.org/10.3322/caac.21559.

(11) Sambasivan, S. Epithelial Ovarian Cancer: Review Article. *Cancer Treat. Res. Commun.* **2022**, *33*, 100629. https://doi.org/10.1016/j.ctarc.2022.100629.

(12) Vang, R.; Shih, I.-M.; Kurman, R. J. Ovarian Low-Grade and High-Grade Serous Carcinoma: Pathogenesis, Clinicopathologic and Molecular Biologic Features, and Diagnostic Problems. *Adv. Anat. Pathol.* **2009**, *16* (5), 267–282. https://doi.org/10.1097/PAP.0b013e3181b4fffa.

(13) Babaier, A.; Mal, H.; Alselwi, W.; Ghatage, P. Low-Grade Serous Carcinoma of the Ovary: The Current Status. *Diagnostics* **2022**, *12* (2), 458. https://doi.org/10.3390/diagnostics12020458.

(14) Nik, N. N.; Vang, R.; Shih, I.-M.; Kurman, R. J. Origin and Pathogenesis of Pelvic (Ovarian, Tubal, and Primary Peritoneal) Serous Carcinoma. *Annu. Rev. Pathol. Mech. Dis.* **2014**, *9* (1), 27–45. https://doi.org/10.1146/annurev-pathol-020712-163949.

(15) Wang, L.; Zhang, Q.; Wang, X.; Dong, Z.; Liu, S.; Wang, Q.; Zhang, Z.; Xing, J. Therapeutic Landscape of Ovarian Cancer: Recent Advances and Emerging Therapies. *Biomark. Res.* **2025**, *13* (1), 103. https://doi.org/10.1186/s40364-025-00818-7.

(16) Novak, C.; Horst, E.; Mehta, G. Review: Mechanotransduction in Ovarian Cancer: Shearing into the Unknown. *APL Bioeng.* **2018**, *2* (3), 031701. https://doi.org/10.1063/1.5024386.

(17) Lheureux, S.; Gourley, C.; Vergote, I.; Oza, A. M. Epithelial Ovarian Cancer. *The Lancet* **2019**, *393* (10177), 1240–1253. https://doi.org/10.1016/S0140-6736(18)32552-2.

(18) Ding, D.-N.; Xie, L.-Z.; Shen, Y.; Li, J.; Guo, Y.; Fu, Y.; Liu, F.-Y.; Han, F.-J. Insights into the Role of Oxidative Stress in Ovarian Cancer. *Oxid. Med. Cell. Longev.* **2021**, *2021* (1), 8388258. https://doi.org/10.1155/2021/8388258.

(19) Adinolfi, S.; Patinen, T.; Jawahar Deen, A.; Pitkänen, S.; Härkönen, J.; Kansanen, E.; Küblbeck, J.; Levonen, A.-L. The KEAP1-NRF2 Pathway: Targets for Therapy and Role in Cancer. *Redox Biol.* **2023**, *63*, 102726. https://doi.org/10.1016/j.redox.2023.102726.
(20) Ma, Q. Role of Nrf2 in Oxidative Stress and Toxicity. *Annu. Rev. Pharmacol. Toxicol.* **2013**, *53* (1), 401–426. https://doi.org/10.1146/annurev-pharmtox-011112-140320.
(21) Buendia, I.; Michalska, P.; Navarro, E.; Gameiro, I.; Egea, J.; León, R. Nrf2–ARE Pathway: An Emerging Target against Oxidative Stress and Neuroinflammation in Neurodegenerative Diseases. *Pharmacol. Ther.* **2016**, *157*, 84–104. https://doi.org/10.1016/j.pharmthera.2015.11.003.
(22) Kensler, T. W.; Wakabayashi, N. Nrf2: Friend or Foe for Chemoprevention? *Carcinogenesis* **2010**, *31* (1), 90–99. https://doi.org/10.1093/carcin/bgp231.
(23) Martinez, A.; Buckley, M.; Scalise, C. B.; Katre, A. A.; Dholakia, J. J.; Crossman, D.; Birrer, M. J.; Berry, J. L.; Arend, R. C. Understanding the Effect of Mechanical Forces on Ovarian Cancer Progression. *Gynecol. Oncol.* **2021**, *162* (1), 154–162. https://doi.org/10.1016/j.ygyno.2021.04.003.
(24) Hernansanz-Agustín, P.; Enríquez, J. A. Generation of Reactive Oxygen Species by Mitochondria. *Antioxidants* **2021**, *10* (3), 415. https://doi.org/10.3390/antiox10030415.
(25) Murphy, M. P. How Mitochondria Produce Reactive Oxygen Species. *Biochem. J.* **2009**, *417* (1), 1–13. https://doi.org/10.1042/BJ20081386.
(26) Dan Dunn, J.; Alvarez, L. A.; Zhang, X.; Soldati, T. Reactive Oxygen Species and Mitochondria: A Nexus of Cellular Homeostasis. *Redox Biol.* **2015**, *6*, 472–485. https://doi.org/10.1016/j.redox.2015.09.005.
(27) Sies, H.; Jones, D. P. Reactive Oxygen Species (ROS) as Pleiotropic Physiological Signalling Agents. *Nat. Rev. Mol. Cell Biol.* **2020**, *21* (7), 363–383. https://doi.org/10.1038/s41580-020-0230-3.
(28) Hayes, J. D.; Dinkova-Kostova, A. T.; Tew, K. D. Oxidative Stress in Cancer. *Cancer Cell* **2020**, *38* (2), 167–197. https://doi.org/10.1016/j.ccell.2020.06.001.
(29) Markesbery, W. R. The Role of Oxidative Stress in Alzheimer Disease. *Arch. Neurol.* **1999**, *56* (12), 1449. https://doi.org/10.1001/archneur.56.12.1449.
(30) Chen, X.; Xie, N.; Feng, L.; Huang, Y.; Wu, Y.; Zhu, H.; Tang, J.; Zhang, Y. Oxidative Stress in Diabetes Mellitus and Its Complications: From Pathophysiology to Therapeutic Strategies. *Chin. Med. J. (Engl.)* **2025**, *138* (1), 15–27. https://doi.org/10.1097/CM9.0000000000003230.
(31) Saed, G. M.; Diamond, M. P.; Fletcher, N. M. Updates of the Role of Oxidative Stress in the Pathogenesis of Ovarian Cancer. *Gynecol. Oncol.* **2017**, *145* (3), 595–602. https://doi.org/10.1016/j.ygyno.2017.02.033.
(32) Lu, J.; Zhang, L.; Xie, F.; Zhu, L.; Li, X.; Ouyang, J.; He, X.; Han, S.; Yi, C. Mild Oxidative Stress Induced by a Low Dose of Cisplatin Contributes to the Escape of TRAIL-Mediated Apoptosis in the Ovarian Cancer SKOV3 Cell Line. *Oncol. Rep.* **2016**, *35* (6), 3427–3434. https://doi.org/10.3892/or.2016.4702.
(33) Meshkovska, Y.; Abramov, A.; Mahira, S.; Thatikonda, S. Understanding the Impact of Oxidative Stress on Ovarian Cancer: Advances in Diagnosis and Treatment. *Future Pharmacol.* **2024**, *4* (3), 651–675. https://doi.org/10.3390/futurepharmacol4030035.
(34) Sunkari, S.; Thatikonda, S.; Pooladanda, V.; Challa, V. S.; Godugu, C. Protective Effects of Ambroxol in Psoriasis like Skin Inflammation: Exploration of Possible Mechanisms. *Int. Immunopharmacol.* **2019**, *71*, 301–312. https://doi.org/10.1016/j.intimp.2019.03.035.
(35) Hecht, F.; Zocchi, M.; Alimohammadi, F.; Harris, I. S. Regulation of Antioxidants in Cancer. *Mol. Cell* **2024**, *84* (1), 23–33. https://doi.org/10.1016/j.molcel.2023.11.001.
(36) Chance, B.; Sies, H.; Boveris, A. Hydroperoxide Metabolism in Mammalian Organs. *Physiol. Rev.* **1979**, *59* (3), 527–605. https://doi.org/10.1152/physrev.1979.59.3.527.
(37) Forman, H. J.; Zhang, H. Targeting Oxidative Stress in Disease: Promise and Limitations of Antioxidant Therapy. *Nat. Rev. Drug Discov.* **2021**, *20* (9), 689–709. https://doi.org/10.1038/s41573-021-00233-1.
(38) Peng, Z.; Geh, E.; Chen, L.; Meng, Q.; Fan, Y.; Sartor, M.; Shertzer, H. G.; Liu, Z.-G.; Puga, A.; Xia, Y. Inhibitor of κB Kinase β Regulates Redox Homeostasis by Controlling the Constitutive Levels of Glutathione. *Mol. Pharmacol.* **2010**, *77* (5), 784–792. https://doi.org/10.1124/mol.109.061424.

(39) Rojo, A. I.; Salinas, M.; Martín, D.; Perona, R.; Cuadrado, A. Regulation of Cu/Zn-Superoxide Dismutase Expression via the Phosphatidylinositol 3 Kinase/Akt Pathway and Nuclear Factor-κB. *J. Neurosci.* **2004**, *24* (33), 7324–7334. https://doi.org/10.1523/JNEUROSCI.2111-04.2004.
(40) Moi, P.; Chan, K.; Asunis, I.; Cao, A.; Kan, Y. W. Isolation of NF-E2-Related Factor 2 (Nrf2), a NF-E2-like Basic Leucine Zipper Transcriptional Activator That Binds to the Tandem NF-E2/AP1 Repeat of the Beta-Globin Locus Control Region. *Proc. Natl. Acad. Sci.* **1994**, *91* (21), 9926–9930. https://doi.org/10.1073/pnas.91.21.9926.
(41) Taguchi, K.; Yamamoto, M. The KEAP1–NRF2 System as a Molecular Target of Cancer Treatment. *Cancers* **2020**, *13* (1), 46. https://doi.org/10.3390/cancers13010046.
(42) M. Owen, J.; J. Dormer, K. The Shear Stress/KLF2/Nrf2/ARE Pathway: A Hemodynamic Defense against Oxidative Stress. In *Blood - Updates on Hemodynamics and Thalassemia*; Seda Artis, A., Ed.; IntechOpen, 2022. https://doi.org/10.5772/intechopen.99566.
(43) Tossetta, G.; Fantone, S.; Montanari, E.; Marzioni, D.; Goteri, G. Role of NRF2 in Ovarian Cancer. *Antioxidants* **2022**, *11* (4), 663. https://doi.org/10.3390/antiox11040663.
(44) Lin, L.; Wu, Q.; Lu, F.; Lei, J.; Zhou, Y.; Liu, Y.; Zhu, N.; Yu, Y.; Ning, Z.; She, T.; Hu, M. Nrf2 Signaling Pathway: Current Status and Potential Therapeutic Targetable Role in Human Cancers. *Front. Oncol.* **2023**, *13*, 1184079. https://doi.org/10.3389/fonc.2023.1184079.
(45) Van Der Wijst, M. G. P.; Huisman, C.; Mposhi, A.; Roelfes, G.; Rots, M. G. Targeting Nrf2 in Healthy and Malignant Ovarian Epithelial Cells: Protection versus Promotion. *Mol. Oncol.* **2015**, *9* (7), 1259–1273. https://doi.org/10.1016/j.molonc.2015.03.003.
(46) Baird, L.; Yamamoto, M. The Molecular Mechanisms Regulating the KEAP1-NRF2 Pathway. *Mol. Cell. Biol.* **2020**, *40* (13), e00099-20. https://doi.org/10.1128/MCB.00099-20.
(47) McMahon, M.; Itoh, K.; Yamamoto, M.; Hayes, J. D. Keap1-Dependent Proteasomal Degradation of Transcription Factor Nrf2 Contributes to the Negative Regulation of Antioxidant Response Element-Driven Gene Expression. *J. Biol. Chem.* **2003**, *278* (24), 21592–21600. https://doi.org/10.1074/jbc.M300931200.
(48) Tong, K. I.; Katoh, Y.; Kusunoki, H.; Itoh, K.; Tanaka, T.; Yamamoto, M. Keap1 Recruits Neh2 through Binding to ETGE and DLG Motifs: Characterization of the Two-Site Molecular Recognition Model. *Mol. Cell. Biol.* **2006**, *26* (8), 2887–2900. https://doi.org/10.1128/MCB.26.8.2887-2900.2006.
(49) Canning, P.; Sorrell, F. J.; Bullock, A. N. Structural Basis of Keap1 Interactions with Nrf2. *Free Radic. Biol. Med.* **2015**, *88*, 101–107. https://doi.org/10.1016/j.freeradbiomed.2015.05.034.
(50) Taguchi, K.; Motohashi, H.; Yamamoto, M. Molecular Mechanisms of the Keap1-Nrf2 Pathway in Stress Response and Cancer Evolution: Molecular Mechanisms of the Keap1-Nrf2 Pathway. *Genes Cells* **2011**, *16* (2), 123–140. https://doi.org/10.1111/j.1365-2443.2010.01473.x.
(51) Holland, R.; Hawkins, A. E.; Eggler, A. L.; Mesecar, A. D.; Fabris, D.; Fishbein, J. C. Prospective Type 1 and Type 2 Disulfides of Keap1 Protein. *Chem. Res. Toxicol.* **2008**, *21* (10), 2051–2060. https://doi.org/10.1021/tx800226m.
(52) Fourquet, S.; Guerois, R.; Biard, D.; Toledano, M. B. Activation of NRF2 by Nitrosative Agents and H2O2 Involves KEAP1 Disulfide Formation. *J. Biol. Chem.* **2010**, *285* (11), 8463–8471. https://doi.org/10.1074/jbc.M109.051714.
(53) Barnes, B. M.; Nelson, L.; Tighe, A.; Burghel, G. J.; Lin, I.-H.; Desai, S.; McGrail, J. C.; Morgan, R. D.; Taylor, S. S. Distinct Transcriptional Programs Stratify Ovarian Cancer Cell Lines into the Five Major Histological Subtypes. *Genome Med.* **2021**, *13* (1), 140. https://doi.org/10.1186/s13073-021-00952-5.
(54) Marinho, H. S.; Real, C.; Cyrne, L.; Soares, H.; Antunes, F. Hydrogen Peroxide Sensing, Signaling and Regulation of Transcription Factors. *Redox Biol.* **2014**, *2*, 535–562. https://doi.org/10.1016/j.redox.2014.02.006.
(55) M. Owen, J.; J. Dormer, K. The Shear Stress/KLF2/Nrf2/ARE Pathway: A Hemodynamic Defense against Oxidative Stress. In *Blood - Updates on Hemodynamics and Thalassemia*; Seda Artis, A., Ed.; IntechOpen, 2022. https://doi.org/10.5772/intechopen.99566.

(56) Mammoto, A.; Mammoto, T.; Ingber, D. E. Mechanosensitive Mechanisms in Transcriptional Regulation. *J. Cell Sci.* **2012**, jcs.093005. https://doi.org/10.1242/jcs.093005.
(57) Di, X.; Gao, X.; Peng, L.; Ai, J.; Jin, X.; Qi, S.; Li, H.; Wang, K.; Luo, D. Cellular Mechanotransduction in Health and Diseases: From Molecular Mechanism to Therapeutic Targets. *Signal Transduct. Target. Ther.* **2023**, *8* (1), 282. https://doi.org/10.1038/s41392-023-01501-9.
(58) De Visser, K. E.; Joyce, J. A. The Evolving Tumor Microenvironment: From Cancer Initiation to Metastatic Outgrowth. *Cancer Cell* **2023**, *41* (3), 374–403. https://doi.org/10.1016/j.ccell.2023.02.016.
(59) Wozniak, M. A.; Chen, C. S. Mechanotransduction in Development: A Growing Role for Contractility. *Nat. Rev. Mol. Cell Biol.* **2009**, *10* (1), 34–43. https://doi.org/10.1038/nrm2592.
(60) Montagner, M.; Dupont, S. Mechanical Forces as Determinants of Disseminated Metastatic Cell Fate. *Cells* **2020**, *9* (1), 250. https://doi.org/10.3390/cells9010250.
(61) Ogawa, R. Mechanobiology and Mechanotherapy in Tissue Engineering. In *In Situ Tissue Regeneration*; Elsevier, 2016; pp 165–181. https://doi.org/10.1016/B978-0-12-802225-2.00009-X.
(62) McSweeney, S. R.; Warabi, E.; Siow, R. C. M. Nrf2 as an Endothelial Mechanosensitive Transcription Factor: Going With the Flow. *Hypertension* **2016**, *67* (1), 20–29. https://doi.org/10.1161/HYPERTENSIONAHA.115.06146.
(63) Fledderus, J. O.; Boon, R. A.; Volger, O. L.; Hurttila, H.; Ylä-Herttuala, S.; Pannekoek, H.; Levonen, A.-L.; Horrevoets, A. J. G. KLF2 Primes the Antioxidant Transcription Factor Nrf2 for Activation in Endothelial Cells. *Arterioscler. Thromb. Vasc. Biol.* **2008**, *28* (7), 1339–1346. https://doi.org/10.1161/ATVBAHA.108.165811.
(64) Dabravolski, S. A.; Sukhorukov, V. N.; Kalmykov, V. A.; Grechko, A. V.; Shakhpazyan, N. K.; Orekhov, A. N. The Role of KLF2 in the Regulation of Atherosclerosis Development and Potential Use of KLF2-Targeted Therapy. *Biomedicines* **2022**, *10* (2), 254. https://doi.org/10.3390/biomedicines10020254.
(65) Pearson, R.; Fleetwood, J.; Eaton, S.; Crossley, M.; Bao, S. Krüppel-like Transcription Factors: A Functional Family. *Int. J. Biochem. Cell Biol.* **2008**, *40* (10), 1996–2001. https://doi.org/10.1016/j.biocel.2007.07.018.
(66) Li, Z.-Y.; Zhu, Y.-X.; Chen, J.-R.; Chang, X.; Xie, Z.-Z. The Role of KLF Transcription Factor in the Regulation of Cancer Progression. *Biomed. Pharmacother.* **2023**, *162*, 114661. https://doi.org/10.1016/j.biopha.2023.114661.
(67) Zhu, M.; Zhang, N.; He, S. Transcription Factor KLF4 Modulates microRNA-106a That Targets Smad7 in Gastric Cancer. *Pathol. - Res. Pract.* **2019**, *215* (8), 152467. https://doi.org/10.1016/j.prp.2019.152467.
(68) Zou, H.; Chen, H.; Zhou, Z.; Wan, Y.; Liu, Z. ATXN3 Promotes Breast Cancer Metastasis by Deubiquitinating KLF4. *Cancer Lett.* **2019**, *467*, 19–28. https://doi.org/10.1016/j.canlet.2019.09.012.
(69) Sweet, D. R.; Lam, C.; Jain, M. K. Evolutionary Protection of Krüppel-Like Factors 2 and 4 in the Development of the Mature Hemovascular System. *Front. Cardiovasc. Med.* **2021**, *8*, 645719. https://doi.org/10.3389/fcvm.2021.645719.
(70) Wu, Z.; Wang, S. Role of Kruppel-like Transcription Factors in Adipogenesis. *Dev. Biol.* **2013**, *373* (2), 235–243. https://doi.org/10.1016/j.ydbio.2012.10.031.
(71) Wang, F.; Zhu, Y.; Huang, Y.; McAvoy, S.; Johnson, W. B.; Cheung, T. H.; Chung, T. K. H.; Lo, K. W. K.; Yim, S. F.; Yu, M. M. Y.; Ngan, H. Y. S.; Wong, Y. F.; Smith, D. I. Transcriptional Repression of WEE1 by Kruppel-like Factor 2 Is Involved in DNA Damage-Induced Apoptosis. *Oncogene* **2005**, *24* (24), 3875–3885. https://doi.org/10.1038/sj.onc.1208546.
(72) Xu, R.; Chen, Y.; Wei, S.; Chen, J. Comprehensive Pan-Cancer Analysis of the Prognostic Role of KLF Transcription Factor 2 (KLF2) in Human Tumors. *OncoTargets Ther.* **2024**, *Volume 17*, 887–904. https://doi.org/10.2147/OTT.S476179.
(73) Zhang, Y.; Yao, C.; Ju, Z.; Jiao, D.; Hu, D.; Qi, L.; Liu, S.; Wu, X.; Zhao, C. Krüppel-like Factors in Tumors: Key Regulators and Therapeutic Avenues. *Front. Oncol.* **2023**, *13*, 1080720. https://doi.org/10.3389/fonc.2023.1080720.
(74) Shigeta, S.; Toyoshima, M.; Kitatani, K.; Ishibashi, M.; Usui, T.; Yaegashi, N. Transferrin Facilitates the Formation of DNA Double-Strand Breaks via Transferrin Receptor 1: The Possible Involvement of

Transferrin in Carcinogenesis of High-Grade Serous Ovarian Cancer. *Oncogene* **2016**, *35* (27), 3577–3586. https://doi.org/10.1038/onc.2015.425.

(75) Brett M., R.; Jennifer B., P.; Thomas A., S.; Brett M., R.; Jennifer B., P.; Thomas A., S. Epidemiology of Ovarian Cancer: A Review. *Cancer Biol. Med.* **2017**, *14* (1), 9–32. https://doi.org/10.20892/j.issn.2095-3941.2016.0084.

(76) Mateescu, B.; Batista, L.; Cardon, M.; Gruosso, T.; De Feraudy, Y.; Mariani, O.; Nicolas, A.; Meyniel, J.-P.; Cottu, P.; Sastre-Garau, X.; Mechta-Grigoriou, F. miR-141 and miR-200a Act on Ovarian Tumorigenesis by Controlling Oxidative Stress Response. *Nat. Med.* **2011**, *17* (12), 1627–1635. https://doi.org/10.1038/nm.2512.

(77) Cho, H.; Kim, K.; Kim, Y.-B.; Kim, H.; No, J. H. Expression Patterns of Nrf2 and Keap1 in Ovarian Cancer Cells and Their Prognostic Role in Disease Recurrence and Patient Survival. *Int. J. Gynecol. Cancer* **2017**, *27* (3), 412–419. https://doi.org/10.1097/IGC.0000000000000908.

(78) Hyler, A. R.; Baudoin, N. C.; Brown, M. S.; Stremler, M. A.; Cimini, D.; Davalos, R. V.; Schmelz, E. M. Fluid Shear Stress Impacts Ovarian Cancer Cell Viability, Subcellular Organization, and Promotes Genomic Instability. *PLOS ONE* **2018**, *13* (3), e0194170. https://doi.org/10.1371/journal.pone.0194170.

(79) Kalluri, R.; Weinberg, R. A. The Basics of Epithelial-Mesenchymal Transition. *J. Clin. Invest.* **2009**, *119* (6), 1420–1428. https://doi.org/10.1172/JCI39104.

(80) Rizvi, I.; Gurkan, U. A.; Tasoglu, S.; Alagic, N.; Celli, J. P.; Mensah, L. B.; Mai, Z.; Demirci, U.; Hasan, T. Flow Induces Epithelial-Mesenchymal Transition, Cellular Heterogeneity and Biomarker Modulation in 3D Ovarian Cancer Nodules. *Proc. Natl. Acad. Sci.* **2013**, *110* (22). https://doi.org/10.1073/pnas.1216989110.

(81) Sun, C.; Yang, X.; Wang, T.; Cheng, M.; Han, Y. Ovarian Biomechanics: From Health to Disease. *Front. Oncol.* **2022**, *11*, 744257. https://doi.org/10.3389/fonc.2021.744257.

(82) Yang, W.; Toffa, S. E.; Lohn, J. W. G.; Seifalian, A. M.; Winslet, M. C. Malignant Ascites Increases the Antioxidant Ability of Human Ovarian (SKOV-3) and Gastric Adenocarcinoma (KATO-III) Cells. *Gynecol. Oncol.* **2005**, *96* (2), 430–438. https://doi.org/10.1016/j.ygyno.2004.10.016.

(83) Wang, Y.; Ma, J.; Shen, H.; Wang, C.; Sun, Y.; Howell, S. B.; Lin, X. Reactive Oxygen Species Promote Ovarian Cancer Progression via the HIF-1α/LOX/E-Cadherin Pathway. *Oncol. Rep.* **2014**, *32* (5), 2150–2158. https://doi.org/10.3892/or.2014.3448.

(84) M. Owen, J.; J. Dormer, K. The Shear Stress/KLF2/Nrf2/ARE Pathway: A Hemodynamic Defense against Oxidative Stress. In *Blood - Updates on Hemodynamics and Thalassemia*; Seda Artis, A., Ed.; IntechOpen, 2022. https://doi.org/10.5772/intechopen.99566.

(85) *SK-OV-3 [SKOV-3; SKOV3] - HTB-77 | ATCC*. https://www.atcc.org. https://www.atcc.org/products/htb-77 (accessed 2025-07-03).

(86) *NIH:OVCAR-3 [OVCAR3] - HTB-161 | ATCC*. https://www.atcc.org. https://www.atcc.org/products/htb-161 (accessed 2025-07-03).

(87) Fang, I.-J.; Trewyn, B. G. Application of Mesoporous Silica Nanoparticles in Intracellular Delivery of Molecules and Proteins. In *Methods in Enzymology*; Elsevier, 2012; Vol. 508, pp 41–59. https://doi.org/10.1016/B978-0-12-391860-4.00003-3.

(88) Karasová, M.; Jobst, M.; Framke, D.; Bergen, J.; Meier-Menches, S.; Keppler, B.; Koellensperger, G.; Zanghellini, J.; Gerner, C.; Del Favero, G. Mechanical Cues Rewire Lipid Metabolism and Support Chemoresistance in Epithelial Ovarian Cancer Cell Lines OVCAR3 and SKOV3. *Cell Commun. Signal.* **2025**, *23* (1), 193. https://doi.org/10.1186/s12964-025-02144-9.

(89) Avraham-Chakim, L.; Elad, D.; Zaretsky, U.; Kloog, Y.; Jaffa, A.; Grisaru, D. Fluid-Flow Induced Wall Shear Stress and Epithelial Ovarian Cancer Peritoneal Spreading. *PLoS ONE* **2013**, *8* (4), e60965. https://doi.org/10.1371/journal.pone.0060965.

(90) Jarolim, K.; Del Favero, G.; Pahlke, G.; Dostal, V.; Zimmermann, K.; Heiss, E.; Ellmer, D.; Stark, T. D.; Hofmann, T.; Marko, D. Activation of the Nrf2-ARE Pathway by the Alternaria Alternata Mycotoxins Altertoxin I and II. *Arch. Toxicol.* **2017**, *91* (1), 203–216. https://doi.org/10.1007/s00204-016-1726-7.

(91) Grgic, D.; Betschler, A.; Früholz, R.; Novak, B.; Varga, E.; Marko, D. Estrogenic in Vitro Evaluation of Zearalenone and Its Phase I and II Metabolites in Combination with Soy Isoflavones. *Arch. Toxicol.* **2022**, *96* (12), 3385–3402. https://doi.org/10.1007/s00204-022-03358-3.
(92) Niles, A. L.; Moravec, R. A.; Riss, T. L. In Vitro Viability and Cytotoxicity Testing and Same-Well Multi-Parametric Combinations for High Throughput Screening. *Curr. Chem. Genomics* **2009**, *3*, 33–41. https://doi.org/10.2174/1875397300903010033.
(93) Skehan, P.; Storeng, R.; Scudiero, D.; Monks, A.; McMahon, J.; Vistica, D.; Warren, J. T.; Bokesch, H.; Kenney, S.; Boyd, M. R. New Colorimetric Cytotoxicity Assay for Anticancer-Drug Screening. *JNCI J. Natl. Cancer Inst.* **1990**, *82* (13), 1107–1112. https://doi.org/10.1093/jnci/82.13.1107.
(94) Lindemann, K.; Gibbs, E.; Åvall-Lundqvist, E.; dePont Christensen, R.; Woie, K.; Kalling, M.; Auranen, A.; Grenman, S.; Hoegberg, T.; Rosenberg, P.; Skeie-Jensen, T.; Hjerpe, E.; Dørum, A.; Gebski, V.; Kristensen, G. Chemotherapy vs Tamoxifen in Platinum-Resistant Ovarian Cancer: A Phase III, Randomised, Multicentre Trial (Ovaresist). *Br. J. Cancer* **2017**, *116* (4), 455–463. https://doi.org/10.1038/bjc.2016.435.
(95) Bileck, A.; Bortel, P.; Kriz, M.; Janker, L.; Kiss, E.; Gerner, C.; Del Favero, G. Inward Outward Signaling in Ovarian Cancer: Morpho-Phospho-Proteomic Profiling Upon Application of Hypoxia and Shear Stress Characterizes the Adaptive Plasticity of OVCAR-3 and SKOV-3 Cells. *Front. Oncol.* **2022**, *11*, 746411. https://doi.org/10.3389/fonc.2021.746411.
(96) Barascu, A.; Le Chalony, C.; Pennarun, G.; Genet, D.; Zaarour, N.; Bertrand, P. Oxydative Stress Alters Nuclear Shape through Lamins Dysregulation: A Route to Senescence. *Nucleus* **2012**, *3* (5), 411–417. https://doi.org/10.4161/nucl.21674.
(97) Covas, G.; Marinho, H. S.; Cyrne, L.; Antunes, F. Activation of Nrf2 by H2O2. In *Methods in Enzymology*; Elsevier, 2013; Vol. 528, pp 157–171. https://doi.org/10.1016/B978-0-12-405881-1.00009-4.
(98) Tossetta, G.; Marzioni, D. Natural and Synthetic Compounds in Ovarian Cancer: A Focus on NRF2/KEAP1 Pathway. *Pharmacol. Res.* **2022**, *183*, 106365. https://doi.org/10.1016/j.phrs.2022.106365.
(99) Khalil, H. S.; Goltsov, A.; Langdon, S. P.; Harrison, D. J.; Bown, J.; Deeni, Y. Quantitative Analysis of NRF2 Pathway Reveals Key Elements of the Regulatory Circuits Underlying Antioxidant Response and Proliferation of Ovarian Cancer Cells. *J. Biotechnol.* **2015**, *202*, 12–30. https://doi.org/10.1016/j.jbiotec.2014.09.027.
(100) Cullingford, T. E.; Butler, M. J.; Marshall, A. K.; Tham, E. L.; Sugden, P. H.; Clerk, A. Differential Regulation of Krüppel-like Factor Family Transcription Factor Expression in Neonatal Rat Cardiac Myocytes: Effects of Endothelin-1, Oxidative Stress and Cytokines. *Biochim. Biophys. Acta BBA - Mol. Cell Res.* **2008**, *1783* (6), 1229–1236. https://doi.org/10.1016/j.bbamcr.2008.03.007.
(101) Fledderus, J. O.; Boon, R. A.; Volger, O. L.; Hurttila, H.; Ylä-Herttuala, S.; Pannekoek, H.; Levonen, A.-L.; Horrevoets, A. J. G. KLF2 Primes the Antioxidant Transcription Factor Nrf2 for Activation in Endothelial Cells. *Arterioscler. Thromb. Vasc. Biol.* **2008**, *28* (7), 1339–1346. https://doi.org/10.1161/ATVBAHA.108.165811.
(102) Hong, Y.; Sun, Y.; Ainiwaer, M.; Xiao, B.; Zhang, S.; Ning, L.; Zhu, X.; Ji, Y. A Role for YAP / FOXM1 /Nrf2 Axis in Oxidative Stress and Apoptosis of Cataract Induced by UVB Irradiation. *FASEB J.* **2024**, *38* (14), e23832. https://doi.org/10.1096/fj.202400848R.
(103) Ciamporcero, E.; Daga, M.; Pizzimenti, S.; Roetto, A.; Dianzani, C.; Compagnone, A.; Palmieri, A.; Ullio, C.; Cangemi, L.; Pili, R.; Barrera, G. Crosstalk between Nrf2 and YAP Contributes to Maintaining the Antioxidant Potential and Chemoresistance in Bladder Cancer. *Free Radic. Biol. Med.* **2018**, *115*, 447–457. https://doi.org/10.1016/j.freeradbiomed.2017.12.005.
(104) Barrera, G.; Cucci, M. A.; Grattarola, M.; Pizzimenti, S. Nrf2, YAP, Antioxidant Potential, and Cancer. In *Cancer*; Elsevier, 2021; pp 159–170. https://doi.org/10.1016/B978-0-12-819547-5.00015-8.
(105) Bao, L.; Wu, J.; Dodson, M.; Rojo De La Vega, E. M.; Ning, Y.; Zhang, Z.; Yao, M.; Zhang, D. D.; Xu, C.; Yi, X. *ABCF2* , an Nrf2 Target Gene, Contributes to Cisplatin Resistance in Ovarian Cancer Cells. *Mol. Carcinog.* **2017**, *56* (6), 1543–1553. https://doi.org/10.1002/mc.22615.

(106) Shim, G.; Manandhar, S.; Shin, D.; Kim, T.-H.; Kwak, M.-K. Acquisition of Doxorubicin Resistance in Ovarian Carcinoma Cells Accompanies Activation of the NRF2 Pathway. *Free Radic. Biol. Med.* **2009**, *47* (11), 1619–1631. https://doi.org/10.1016/j.freeradbiomed.2009.09.006.
(107) Bao, L.-J.; Jaramillo, M. C.; Zhang, Z.-B.; Zheng, Y.-X.; Yao, M.; Zhang, D. D.; Yi, X.-F. Nrf2 Induces Cisplatin Resistance through Activation of Autophagy in Ovarian Carcinoma. *Int. J. Clin. Exp. Pathol.* **2014**, *7* (4), 1502–1513.
(108) Konstantinopoulos, P. A.; Spentzos, D.; Fountzilas, E.; Francoeur, N.; Sanisetty, S.; Grammatikos, A. P.; Hecht, J. L.; Cannistra, S. A. Keap1 Mutations and Nrf2 Pathway Activation in Epithelial Ovarian Cancer. *Cancer Res.* **2011**, *71* (15), 5081–5089. https://doi.org/10.1158/0008-5472.CAN-10-4668.
(109) Ali, T.; Li, D.; Ponnamperumage, T. N. F.; Peterson, A. K.; Pandey, J.; Fatima, K.; Brzezinski, J.; Jakusz, J. A. R.; Gao, H.; Koelsch, G. E.; Murugan, D. S.; Peng, X. Generation of Hydrogen Peroxide in Cancer Cells: Advancing Therapeutic Approaches for Cancer Treatment. *Cancers* **2024**, *16* (12), 2171. https://doi.org/10.3390/cancers16122171.

6 Appendix

6.1 List of figures